

Cosmic magnetic fields

connections to particle astrophysics

Philipp Kronberg
University of Toronto

CTA Link Symposium,
Buenos Aires, Argentina,

21 November 2012



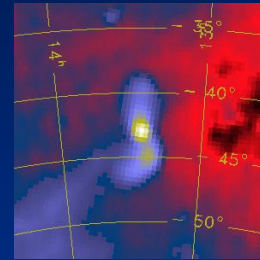
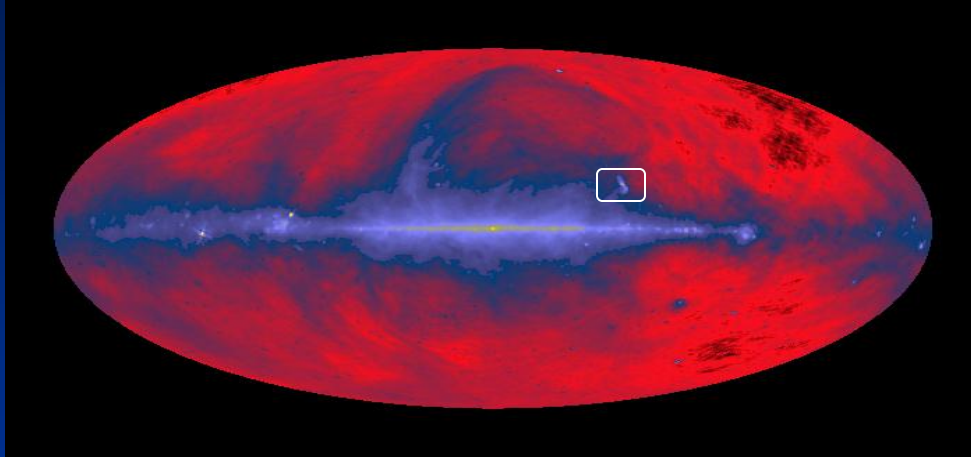
1.

CR propagation models
based on one, or a few prominent UHECR sources

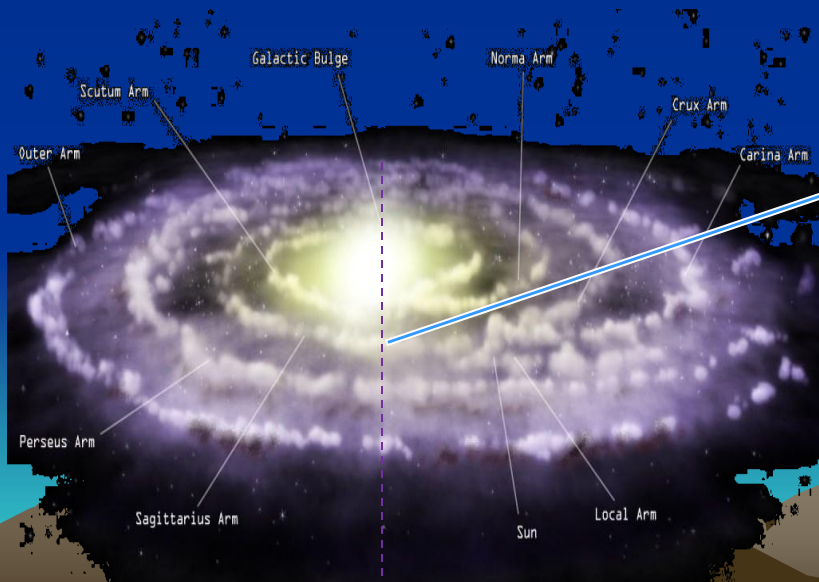
New conceptual for analysis of UHECR propagation.
Initially assume that Cen A is the sole prominent (and
isotropically emitting), local UHECR source)

H. Yüksel, T. Stanev, M. Kistler & P. Kronberg
Astrophysical Journal **758**, 16, 2012 October 10

Geometry: Cen A vs. Milky Way

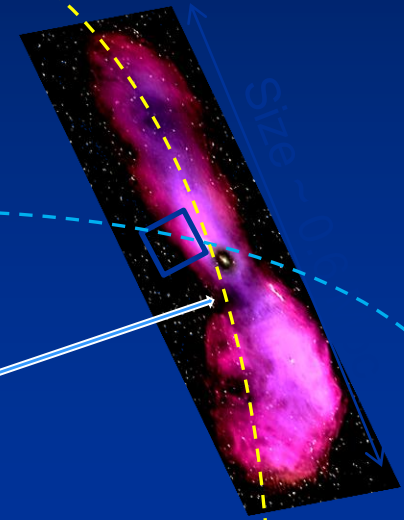


$l \sim 310^\circ$



3.8Mpc

$b \sim 20^\circ$



Cen –A, AUGER + HiRes

A new analysis and conclusions on:

The strength & structure of the nearby EGMF out to ~ 5 Mpc

A comparison of

UHECR simulation and measurement at 1 and 6×10^{19} eV

Yüksel, Stanev, Kistler & Kronberg ApJ **758**, 16, Oct 10 2012

Input UHECR data are from 2010 published data:

AUGER UHECR data: (Argentina)

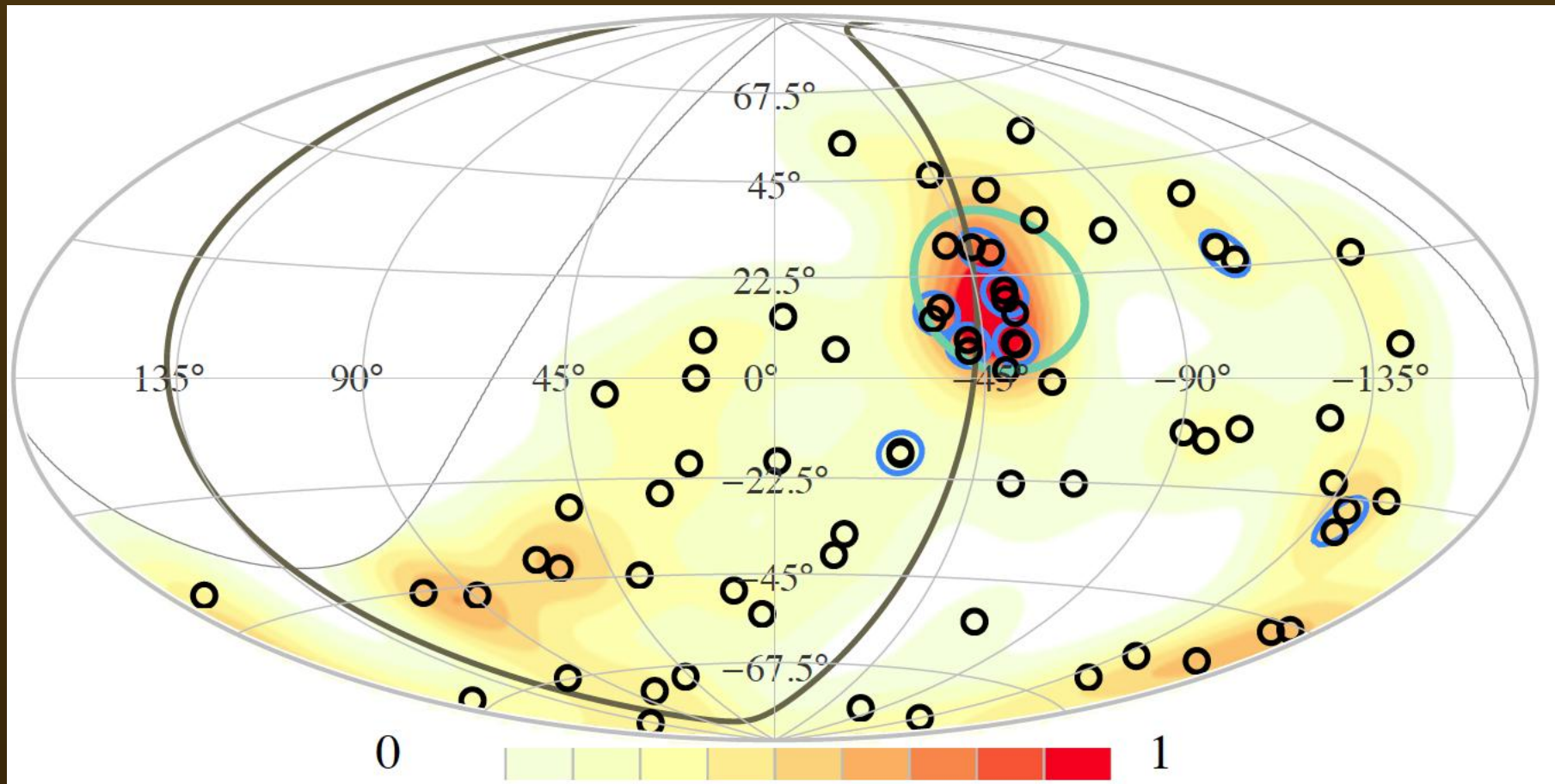
Abreu et al. Astroparticle. Phys. **34**, 314, 2010

HiRes/TA UHECR data: (Utah)

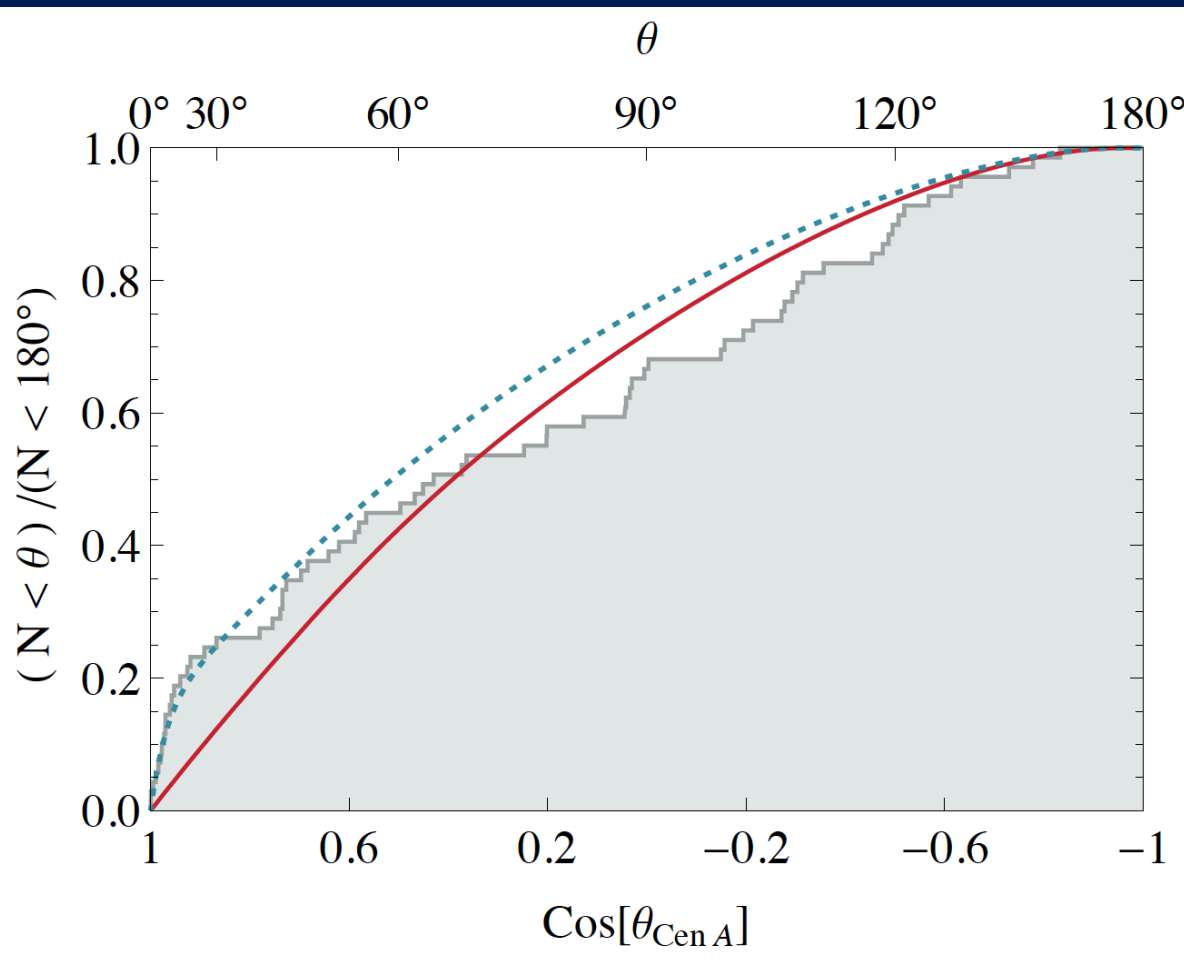
Abbasi R.U. et al., ApJL **713**, L64, 2010

The arrival directions of 69 UHECR events detected by Auger (black circles) in Galactic coordinates. Pairs of events within 5° are shown with blue circles.

A circle of 18° is shown around the radio galaxy Centaurus A. The estimated density distribution of UHECR events are shown with coloured contours



Cumulative angular distribution of events around Cen A



After weighting for exposure, the expectations for

- (solid line)
A purely isotropic distribution of all events
- (dotted blue line)
A model of 10 events from Cen A, smoothed by a 10 degree Gaussian distribution around Cen A -- plus an isotropically distributed 59 events

Even without an excess from the direction of Cen A, the all-sky distribution of events is anisotropic

For a first-order understanding of the angular distribution of events seen by Auger, first look for a range of EGMF parameters that can produce the observed spread of $\sim 10^\circ$ for UHECRs around Cen A's location:
i.e. decide on a useful model framework

Propagation pathlength = d , particle deflection = δ

B_{IG} coherence length = Λ_c shift in arrival direction = θ_{AV} $\theta_{AV} = \frac{\delta_{AV}}{2}$

A: $\Lambda_c \ll d$

B: $\Lambda_c \gg d$

Analytically:

$$\delta_{rms} \simeq 53^\circ \sqrt{1/2} B_{rms} \sqrt{d \Lambda_c} / E$$

$$\theta_{rms} = \delta_{rms} / \sqrt{3}$$

$$\delta_{av} \simeq 53^\circ \sqrt{2/3} B_{rms} d / E$$

$$\theta_{av} = \delta_{av} / 2$$

$$\theta \simeq (\theta_{av}^\eta + \theta_{rms}^\eta)^{1/\eta}$$

$$\simeq 53^\circ \sqrt{1/6} B_{rms} (d/E) \left((\Lambda_c/d)^{\eta/2} + 1 \right)^{1/\eta}$$

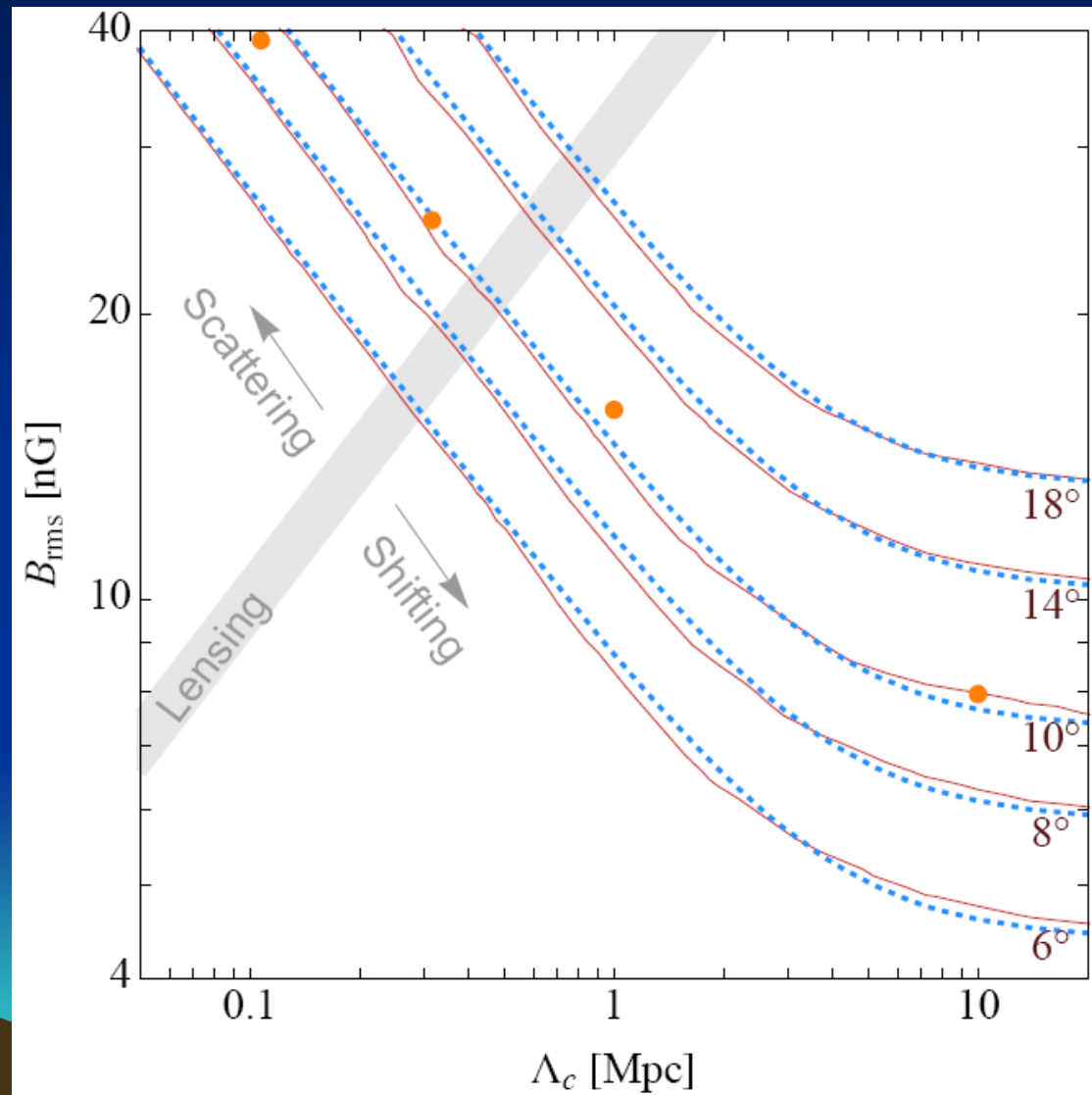
$$\eta \rightarrow -4$$

η parameterizes smoothness of transition from A \rightarrow B

We compute θ numerically, utilizing a fourth-order Runge-Kutta method to solve equation of motion, keeping the step size small in comparison to both the minimum scale of magnetic field variation, and Larmor radius

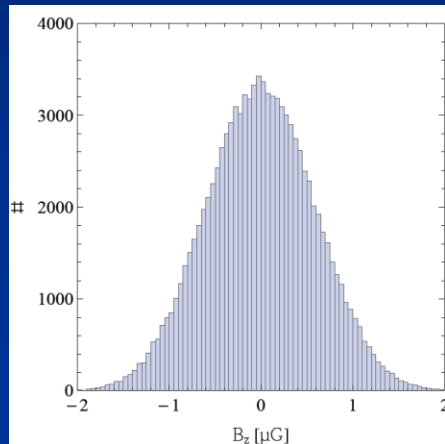
Mean values of cosmic-ray angular distributions for 60 EeV around Centaurus A as a function of field strength and coherence length

- Shown are the expectations from analytical expressions (dotted lines) compared to the our simulation (solid lines)
- Maximum lensing appears in the shaded band

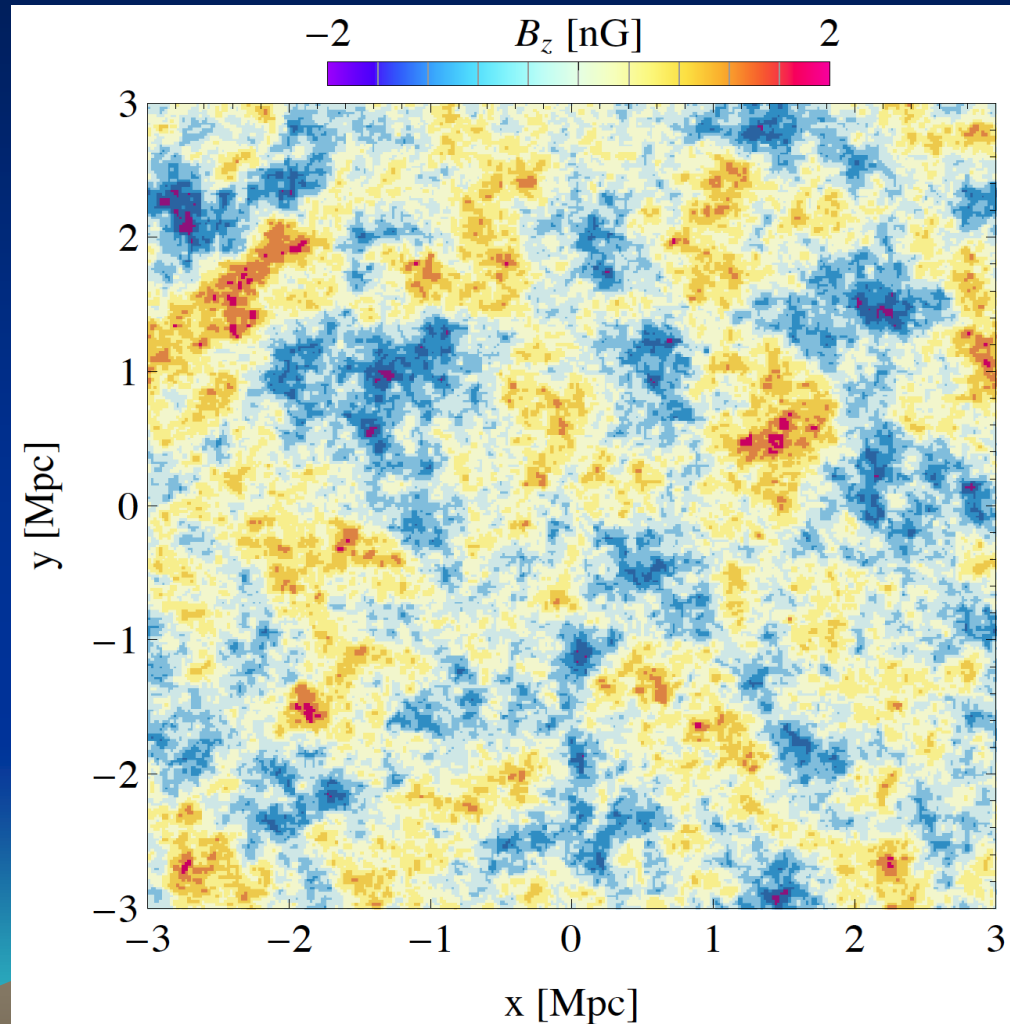


Magnetic Fields

- We generate a divergence free, random magnetic field model whose components have a Gaussian distribution and follow Kolmogorov spectrum



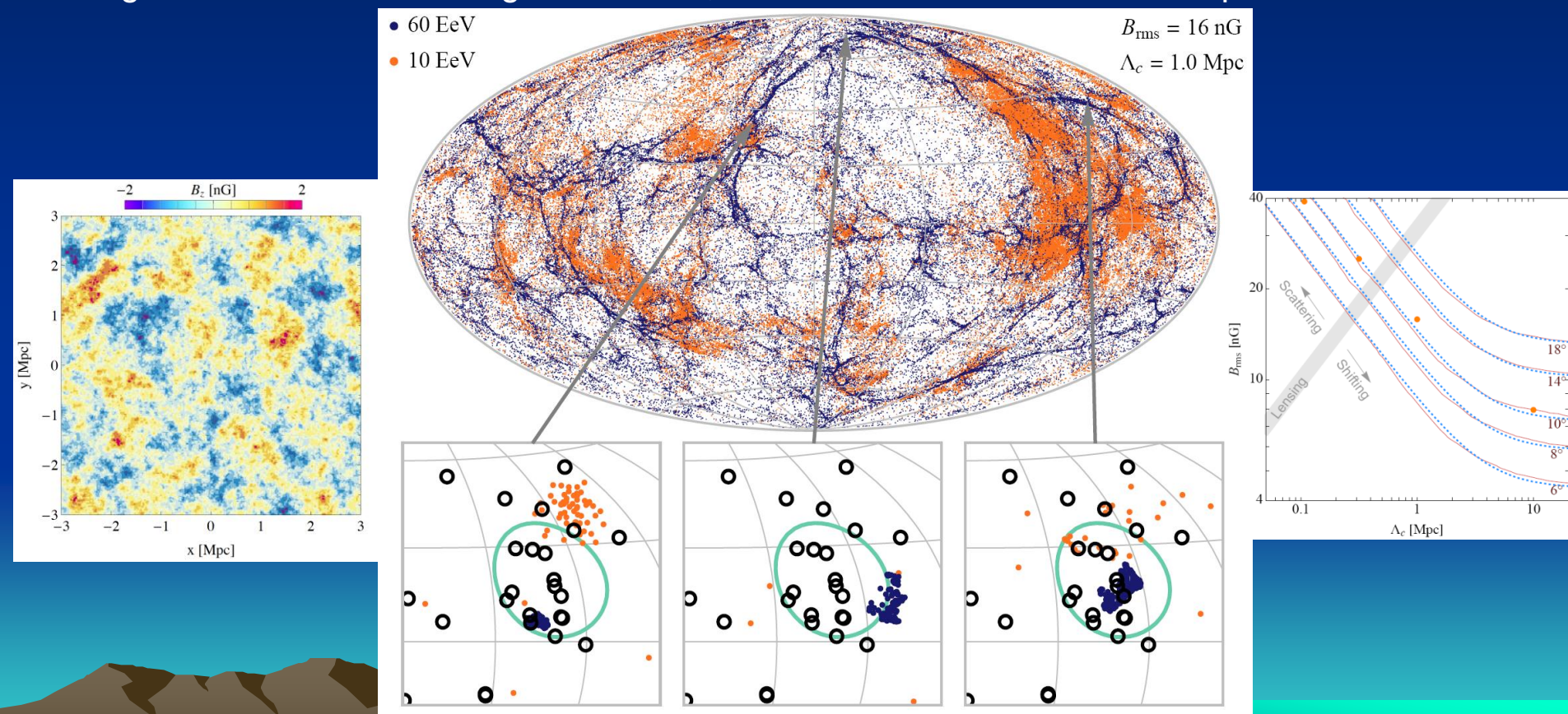
- A slice from the magnetic field simulation. Displays the z component of the field in the x - y plane within a cubic grid of size of 512^3 :

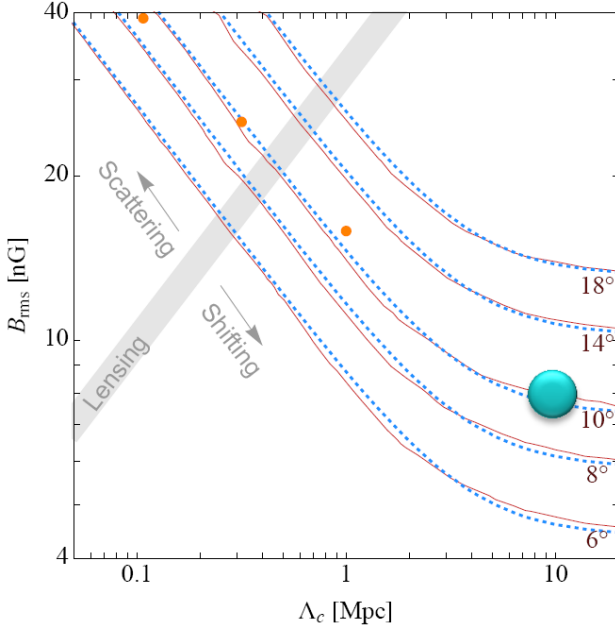


Plausible distributions of cosmic rays are illustrated for a variety of extragalactic magnetic field parametrizations (cosmic rays with energies of **60 EeV (blue)** and **10 EeV (orange)**)

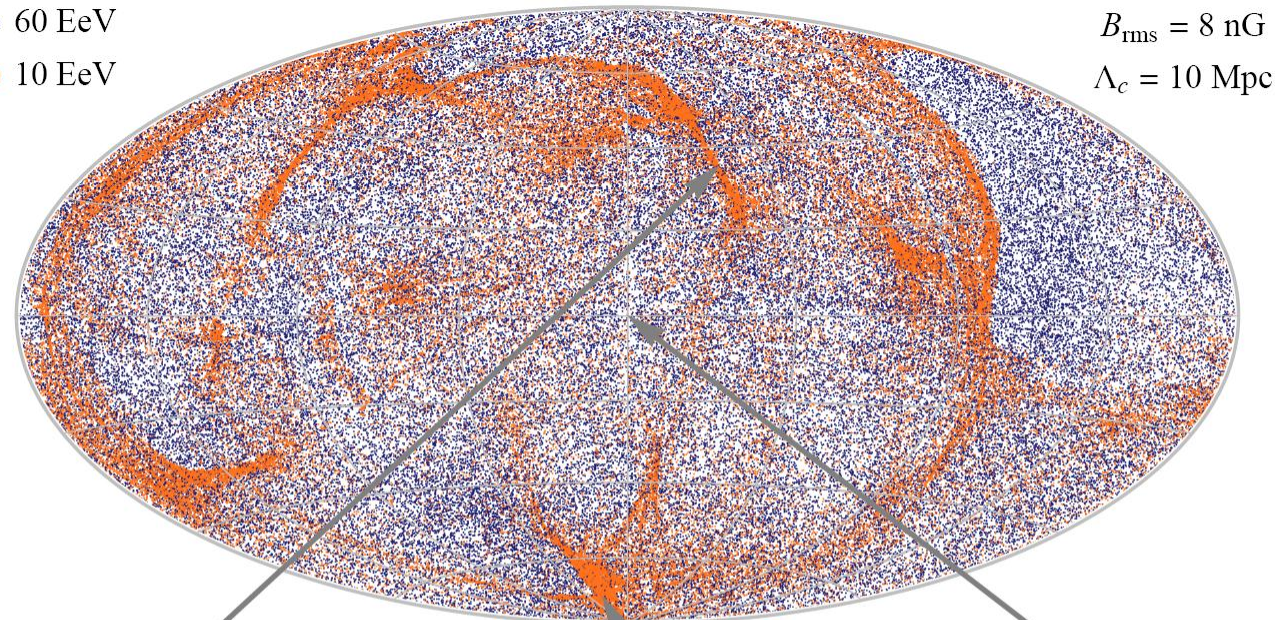
Upper: As seen by an observer located at Cen A, final positions of particles at a distance 3.8 Mpc from the source(100,000 particles are shown for each energy)

Lower: As seen by an Earth-based observer, three characteristic realizations of UHECR angular distributions arriving from Cen A, chosen from locations in the map above



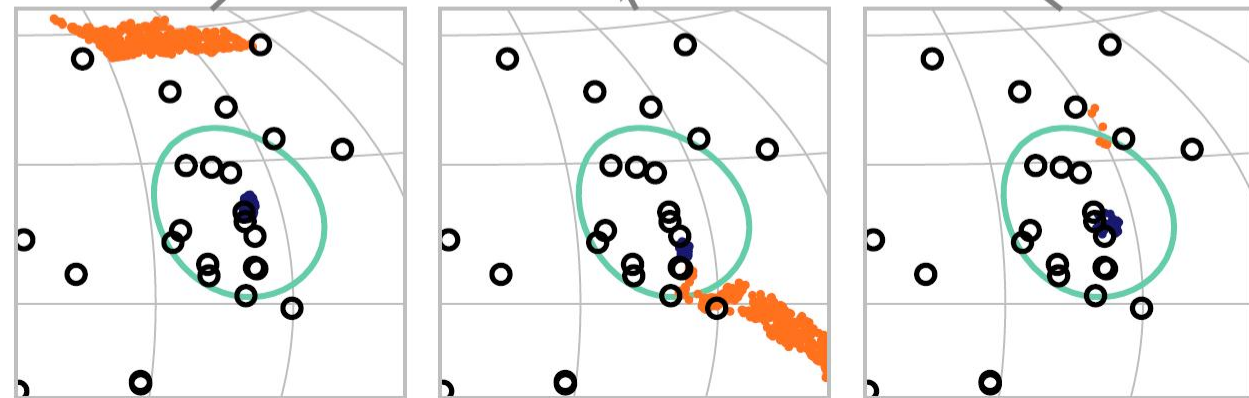


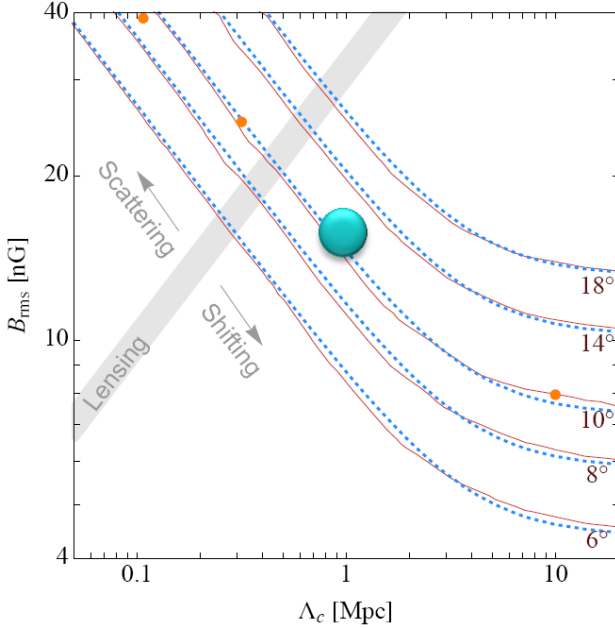
*The sky as seen from Cen A (upper plots)
-- projected on a 3.8 Mpc radius screen*



Lower plots:

*Observed events
vs. (l, b) for the 3 Earth
locations on the
Cen A-centred sphere
above*

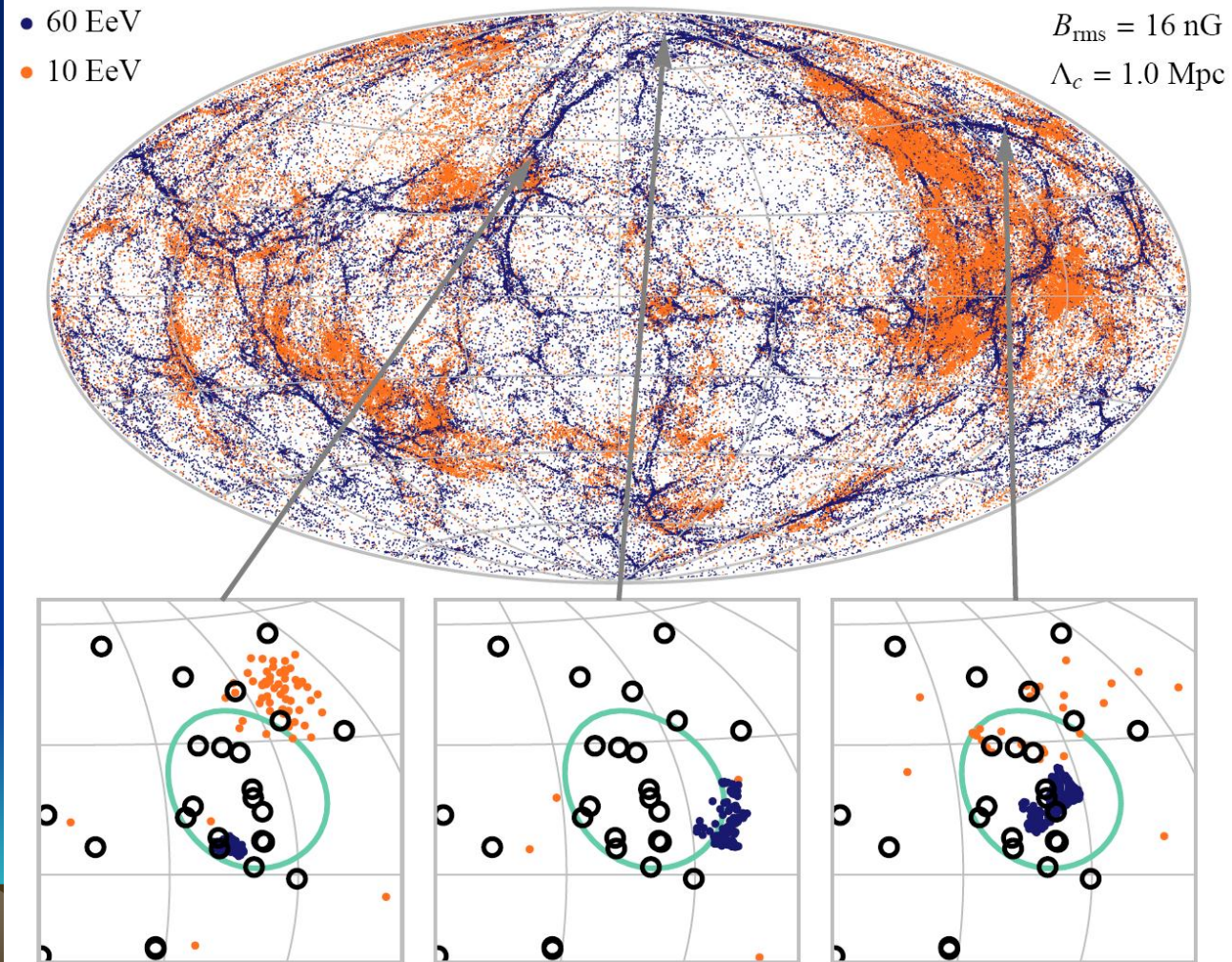




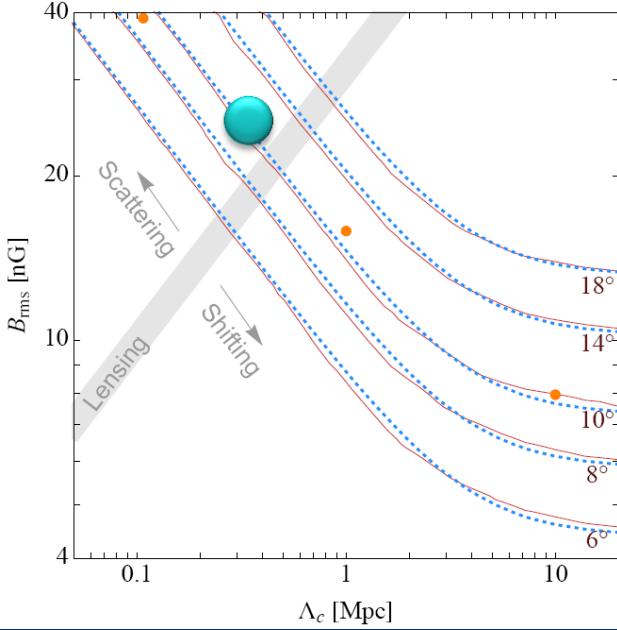
Note the clearly delineated “caustic” zones, here for $E=60$ EeV protons.

These correspond to the gray-shaded “lensing” zone in the upper left inset. They lead to a relatively model - insensitive $\langle B_{IG} \rangle$

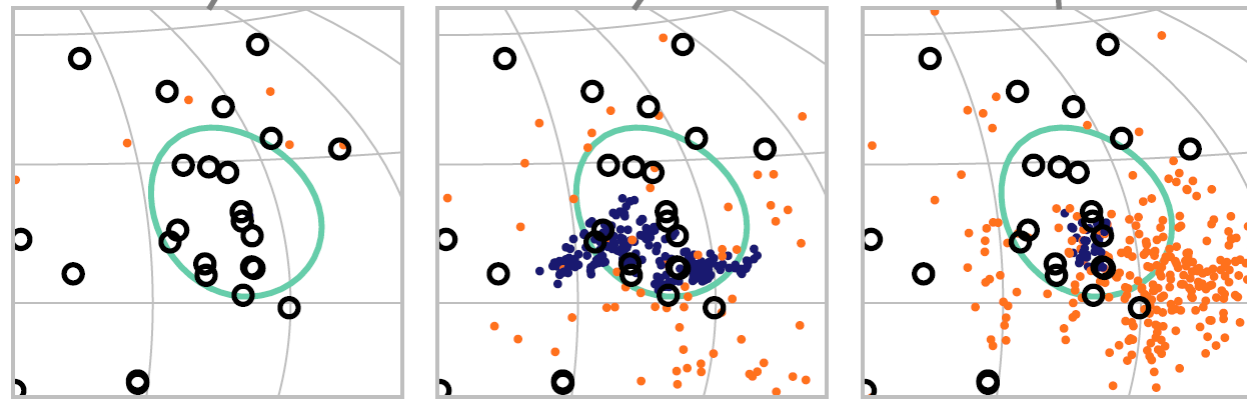
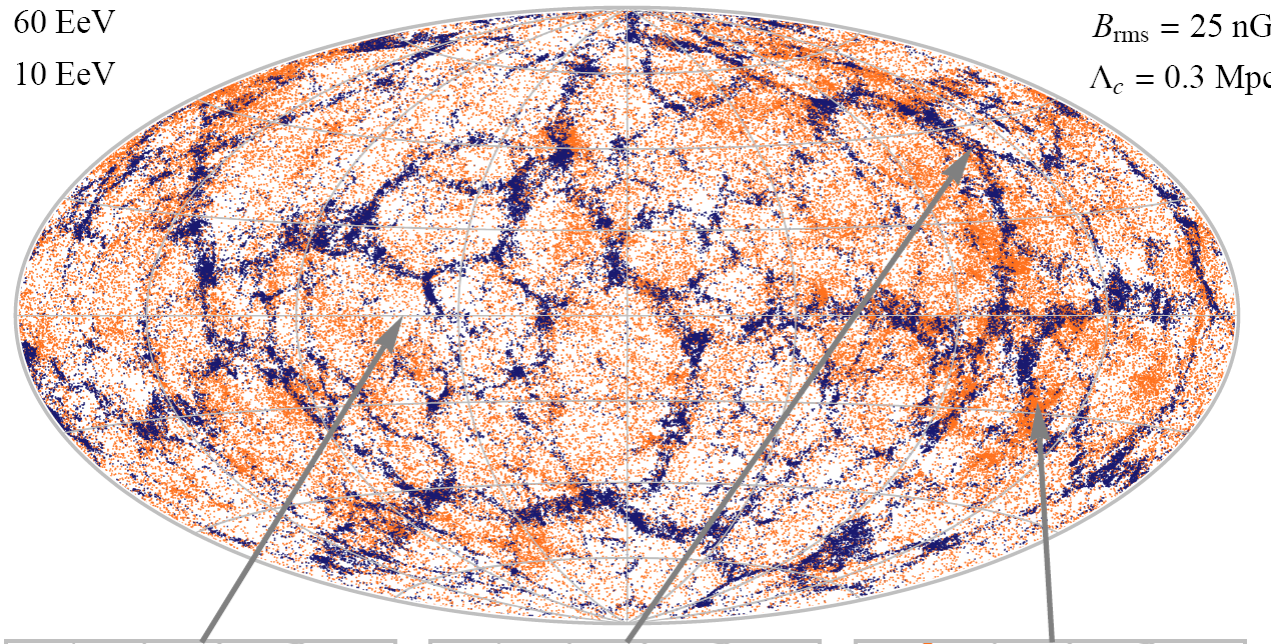
Details in *ApJ* **758**, 16,
(Oct 10) 2012 (Yüksel, Stanev,
Kistler & Kronberg)



b

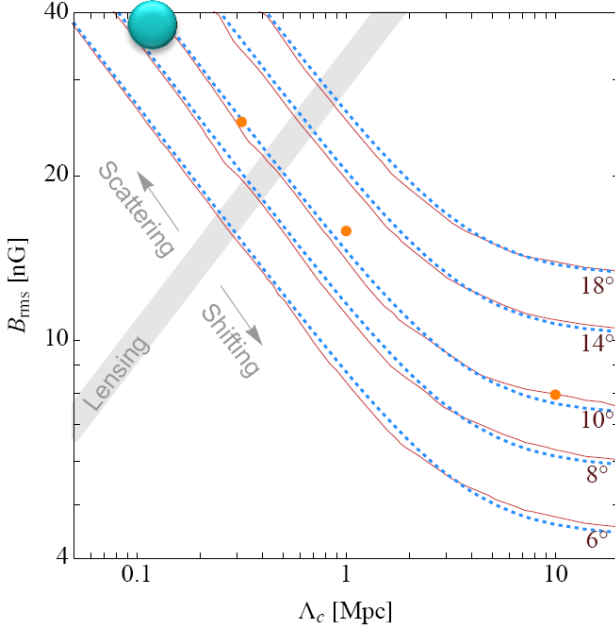


- 60 EeV
- 10 EeV



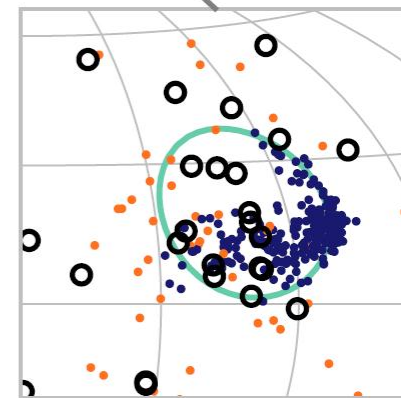
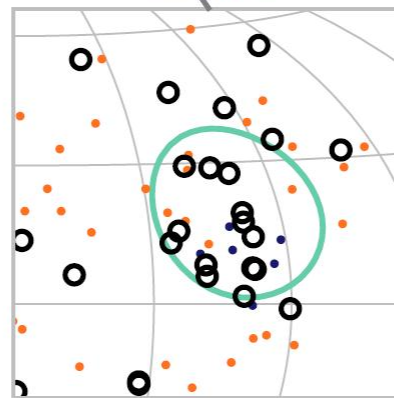
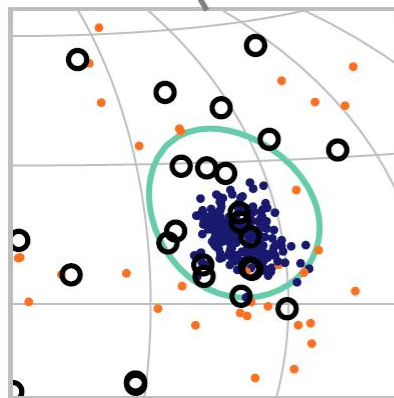
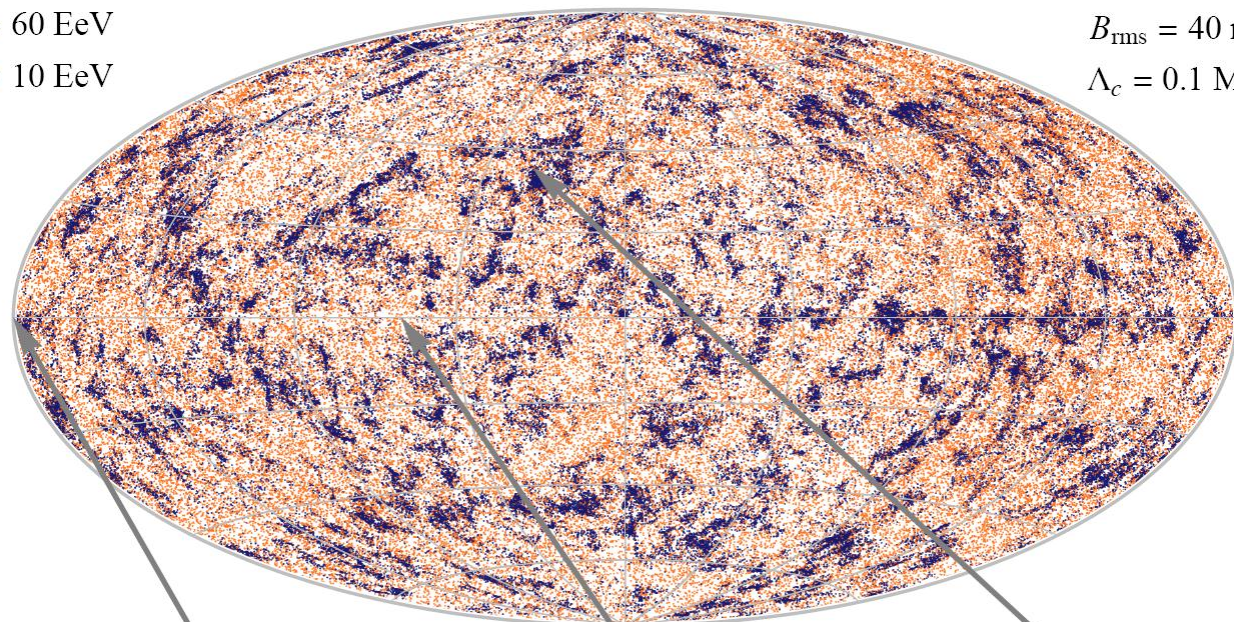
b

l

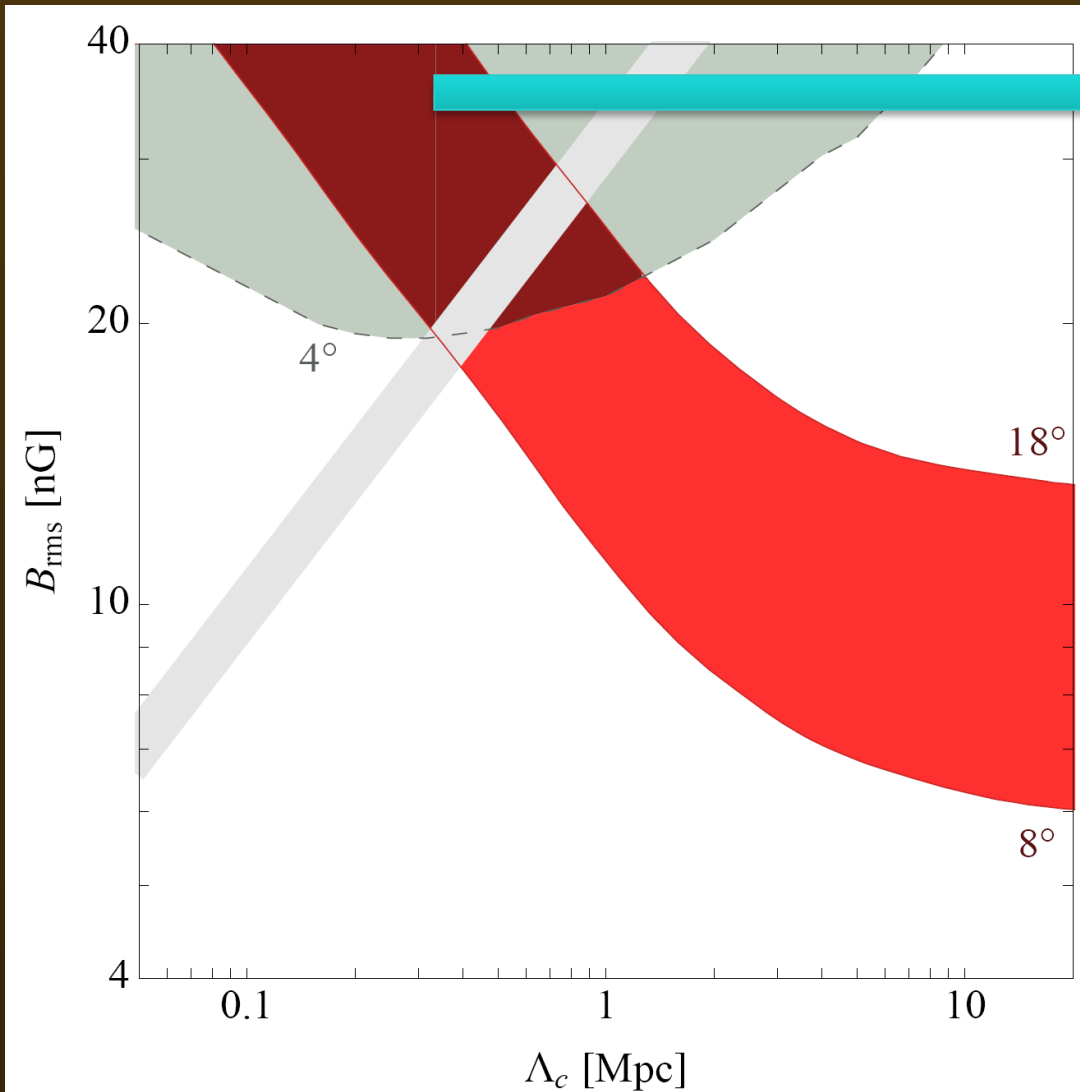


• 60 EeV
• 10 EeV

$B_{\text{rms}} = 40 \text{ nG}$
 $\Lambda_c = 0.1 \text{ Mpc}$



The local Intergalactic Magnetic Field



- Inferred range of extragalactic magnetic field parameters that are compatible with:*

1. the average angular distribution of events $8-18^\circ$ from Cen A (solid lines)

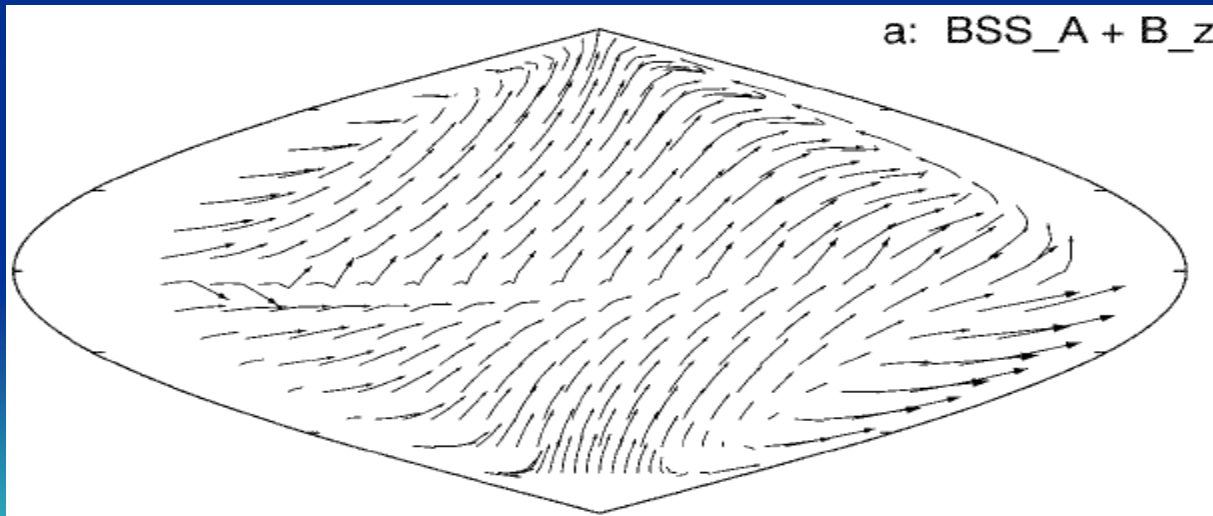
2. the spread of events among themselves is $< 4^\circ$ (dashed line)

Condition 2 disfavors scenarios in which events are shifted from the source position, yet remain tightly clustered

What about the Galactic (Milky Way) magnetic fields?

Not visible in our AUGER UHECR analysis

- GMF in the disk modelled as consisting of two $\sim \mu\text{G}$ strength components :
 - a regular component with reversals in the $\langle B \rangle$ direction between neighboring arms of the galaxy
 - a turbulent component with coherence length of ~ 0.1 kpc
- Protons with energies of 60 EeV expected to be scattered by only about a degree (smaller than the uncertainty of UHECR detectors)
- The regular B -component tends to produce only a coherent shift in the source position:



- We expect the Galactic MF to have only a small effect on protons at the energies examined here and minimally impact our conclusions

What about heavy Nuclei CR's?

- A heavy composition at these energies would imply a flux of protons of the same rigidity for the same trajectories
- We would expect an excess at lower energies, though not as prominent,
- This excess was not seen in the Auger data, so the **simplest interpretation** is a **dominant proton** component. Also suggested by the HiRes measurements from the depth of maximum of the HiRes UHECR showers:



Some Implications:

- A > 10 nG field extending at a few Mpc around the Milky Way results in a ``screen" scattering all UHECR's that eventually reach Earth:
 - each UHECR would then be expected to have a minimum amount of deflection due to this field alone
 - it would increase the difficulty of making associations with more distant sources
 - it would also introduce a minimum time dispersion, important for transient sources, such as gamma-ray bursts

Heavier nuclei plausibly present at the highest obs'd energies

- If it is a solar composition, and acceleration is based on nuclear charge, the observed events near Cen A would suggest 1 or 2 He nuclei in the observed excess.
- *NOTE: The highest energy event seen by Auger --142 EeV and within 30 degree of Cen A, --- is in rough agreement with the high total energy and greater scattering expected for a heavier , e.g. He nucleus*

Variables that can be further explored (resolved) as more UHECR data accumulate in future

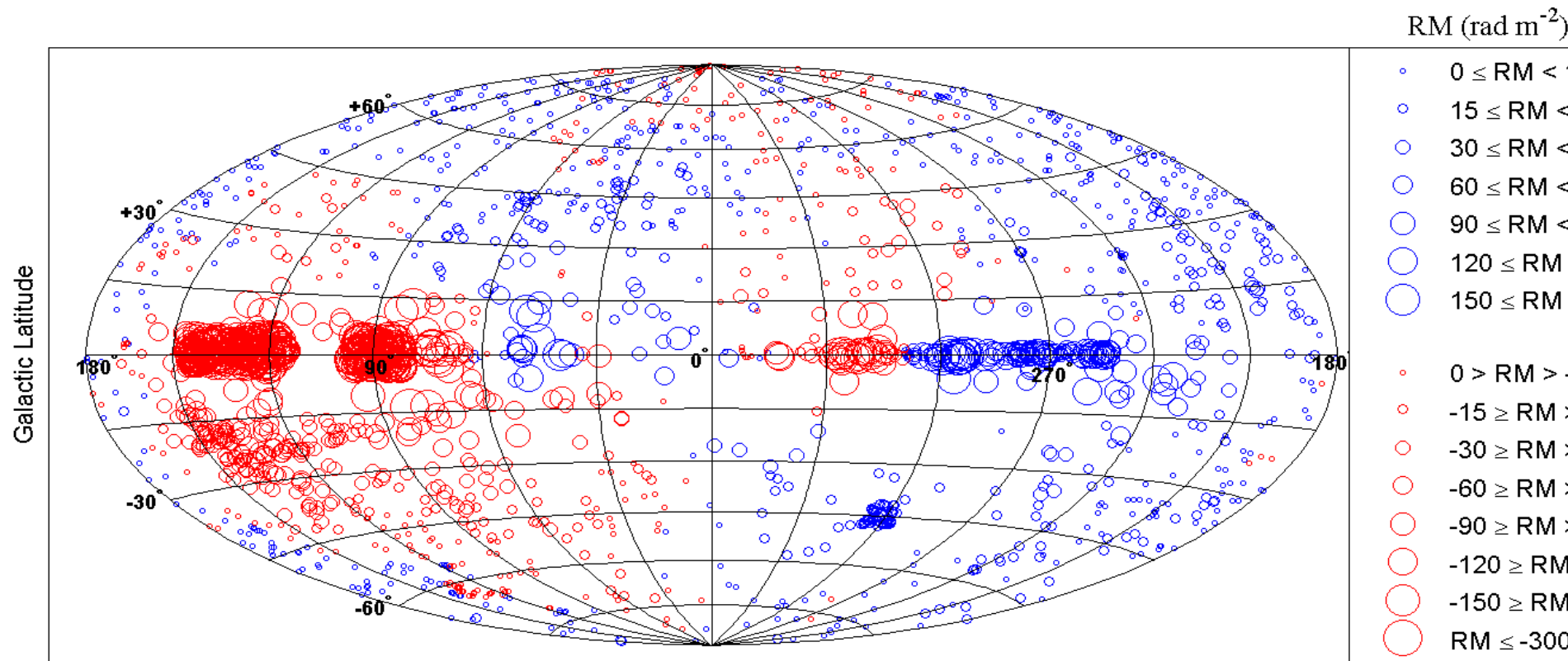
- Better resolution in CR energy (?) – CR lensing → tighter constraints on strength and structure of B_{IG}
- Model with different mixes of CR nucleus composition
e.g. Solar, Fe- dominated, etc.
- Milky Way halo field deflection at lower CR energies
- etc.



- The Milky way is a magnetic “grand design” galaxy



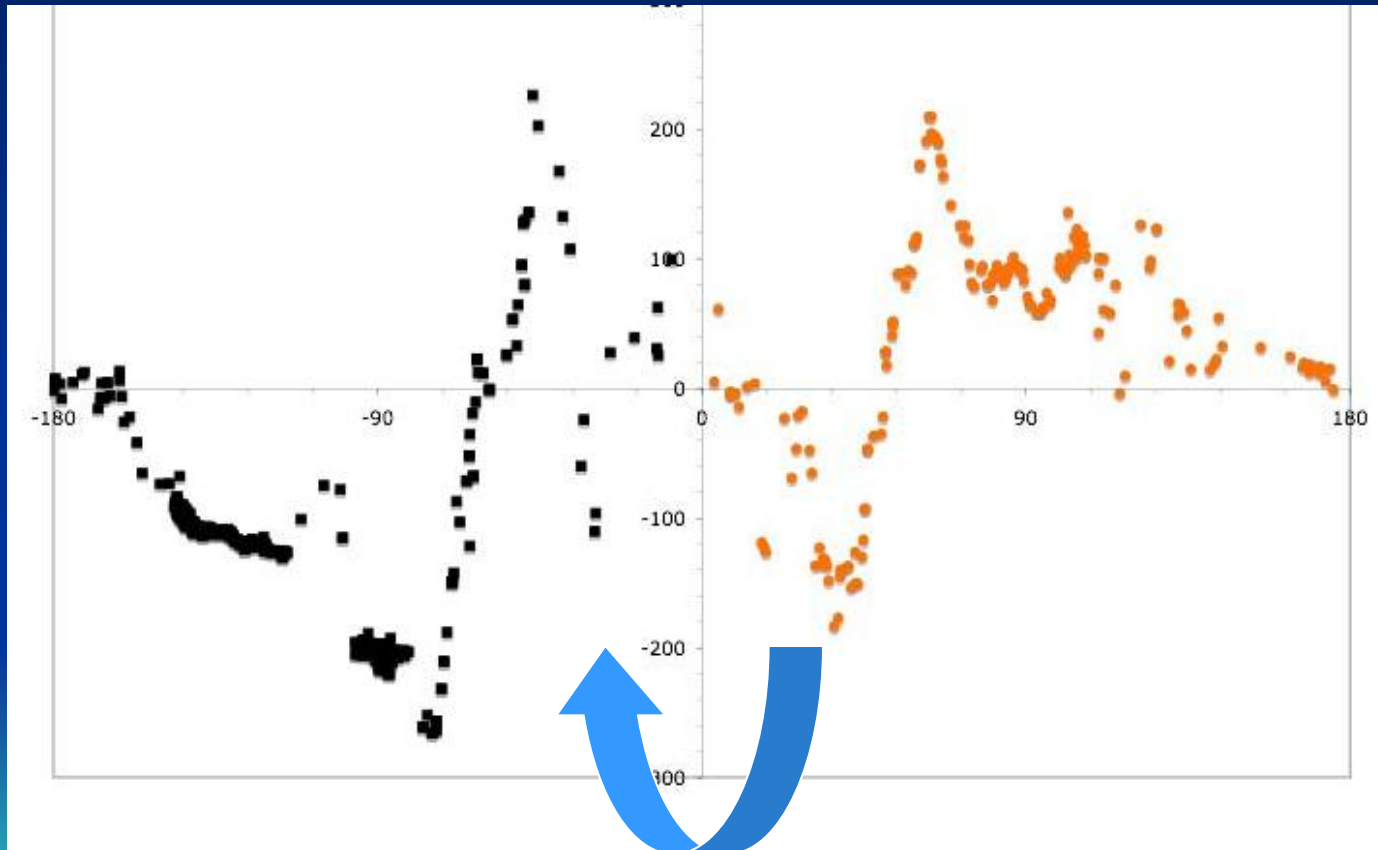
Smoothed Galactic RM sky from 2250 egrs RM's



*P. Kronberg & Katherine J. Newton-McGee, Proc. Ast Soc. Australia **82**, 2011*
Further analysis: M.S.Pshirkov, Tinyakov, Kronberg, Newton-McGee (ApJ 2011)

Smoothed RM's around the Galactic plane at $|b| \leq 10^\circ$ *New evidence for $\langle B \rangle$ in the disk*

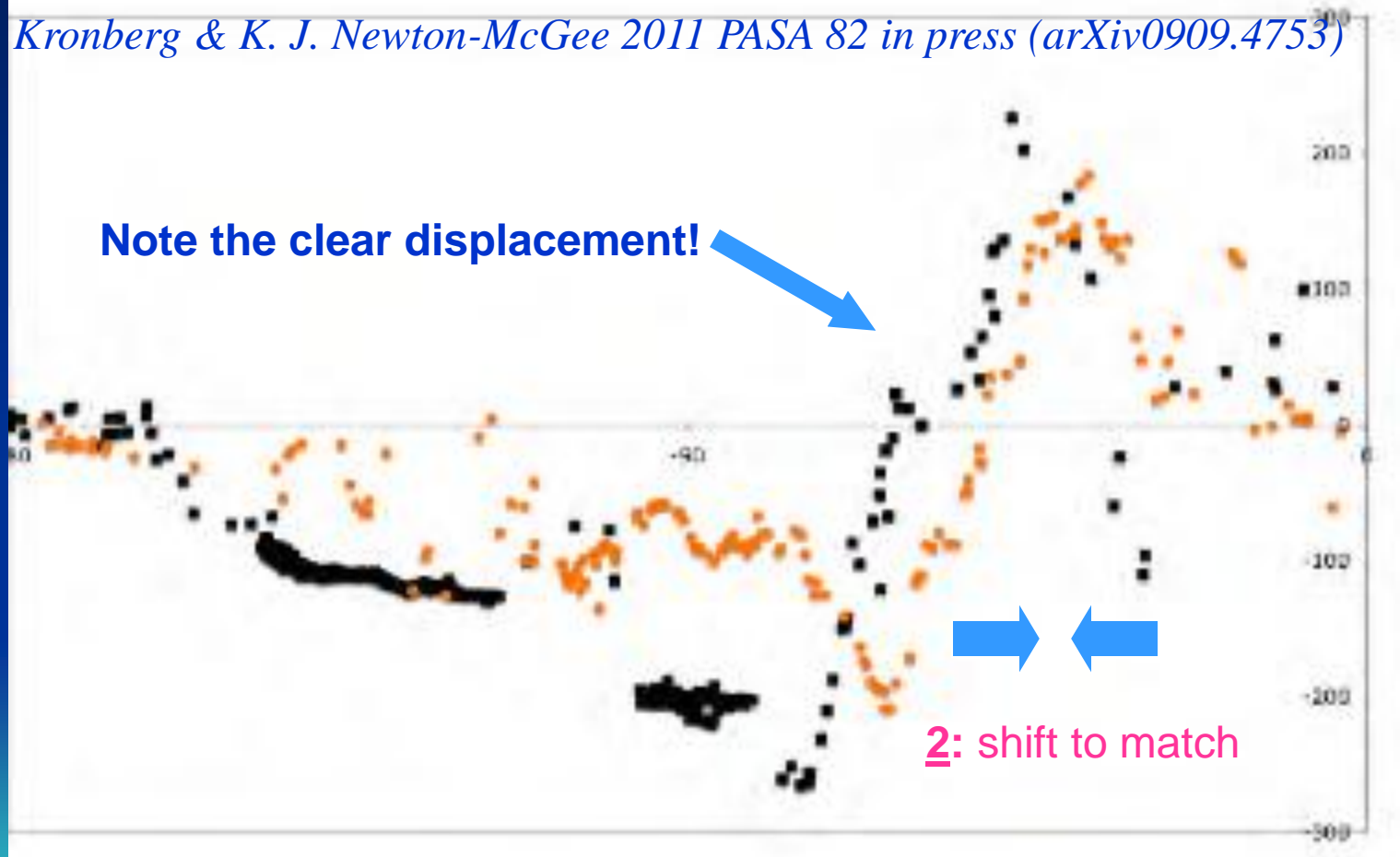
*P.P. Kronberg & K. J. Newton-McGee PASP 2011
(arXiv:0909.4753)*



1. fold about the Galactic center direction ($l=0^\circ$),
and reverse sign

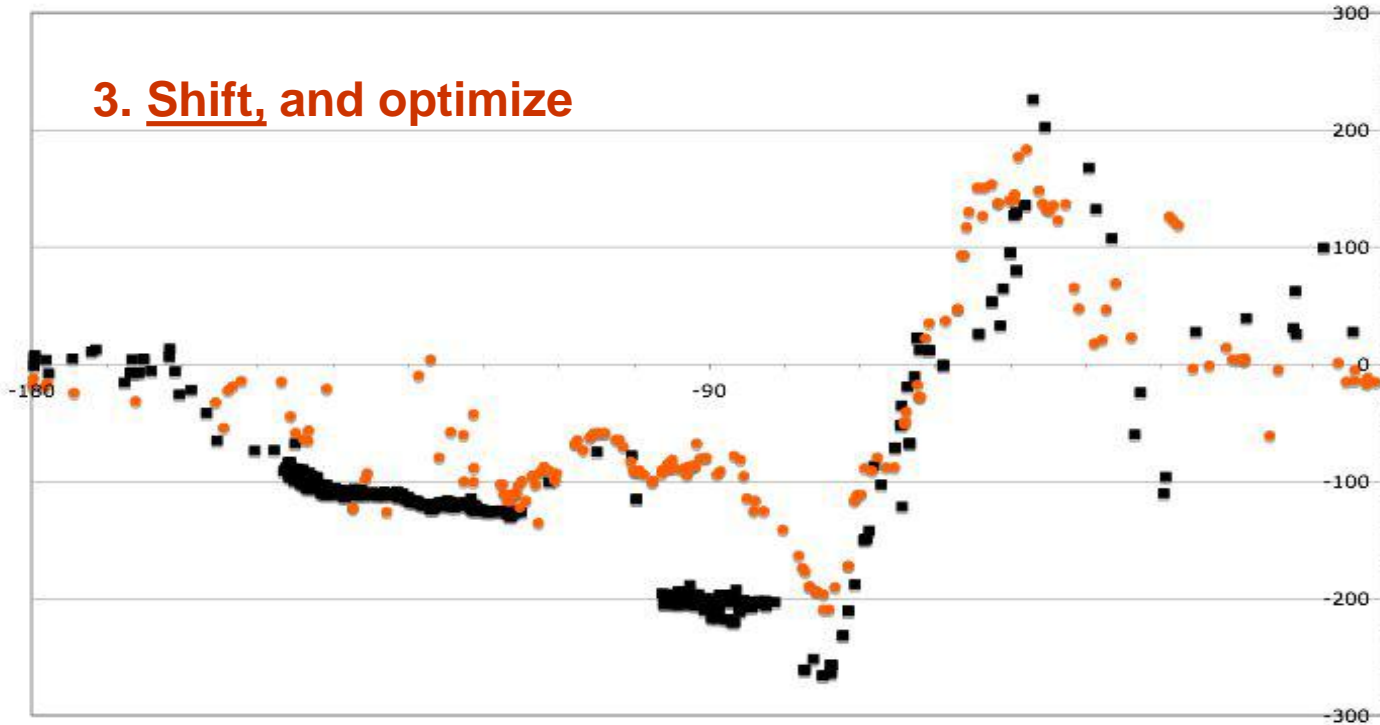
Fold RM's about $l=0$, then reverse the sign
of RM's at $360^\circ > l > 180^\circ$ (orange points)

P.P. Kronberg & K. J. Newton-McGee 2011 PASA 82 in press (arXiv0909.4753)

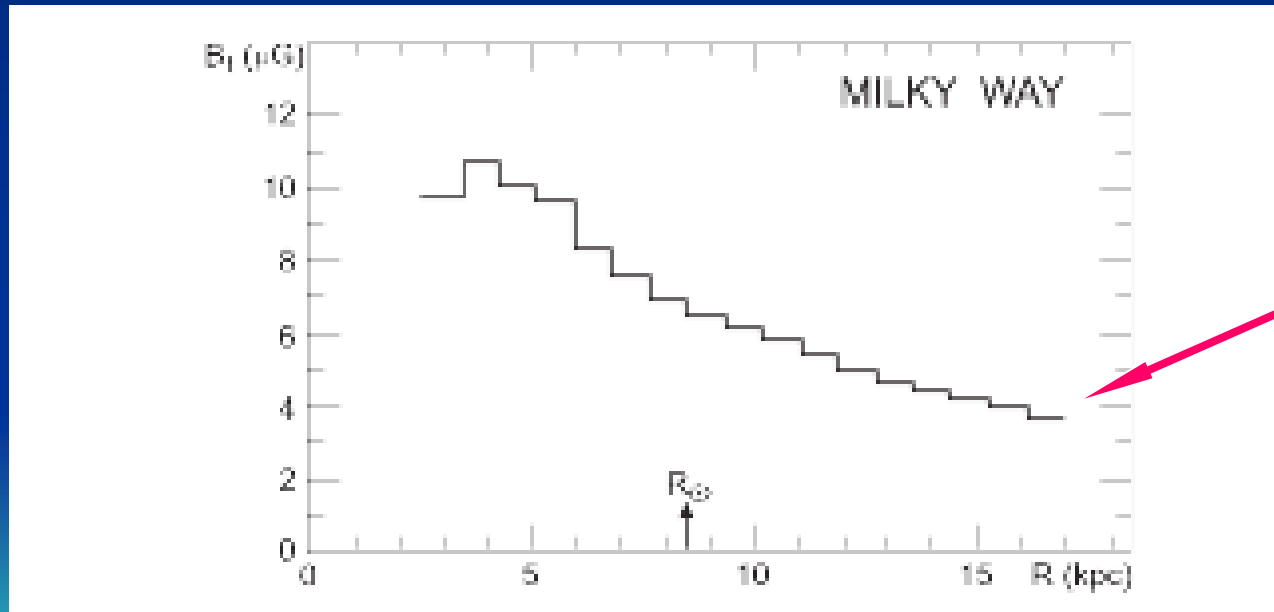


RM's *after* an $11^\circ (\pm 2^\circ)$ shift

3. Shift, and optimize



Model of the Galactic $|B|$ vs. r .
from all-sky, 0.4 GHz synchrotron emissivity
(Haslam, Salter, et al.)
confirmed by γ -ray observations
(Strong et al.)



Connects to
local B_{IGM} ?

Faraday RM probe of magnetic fields in filaments of cosmological LSS

Well-defined Perseus-Pisces
supercluster filament



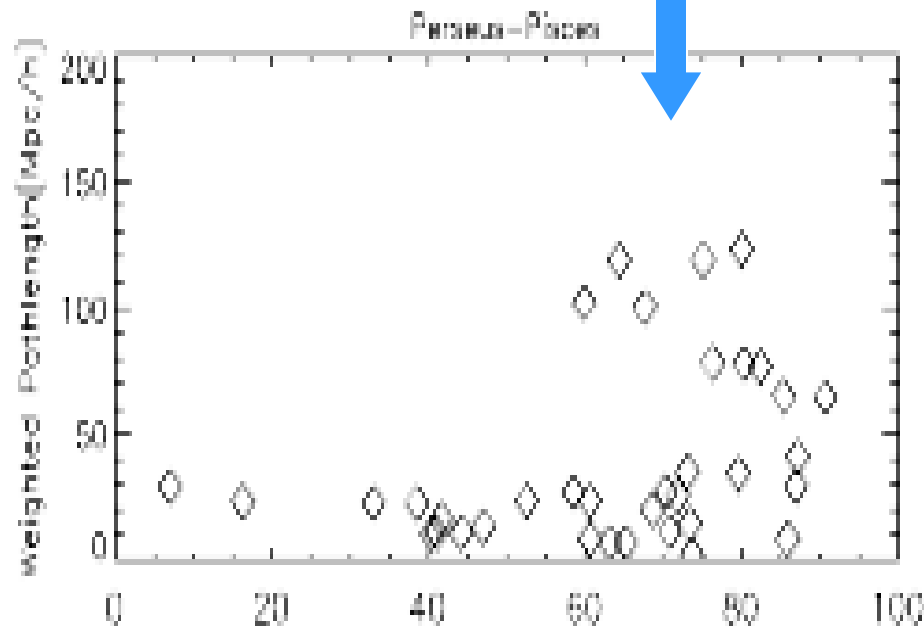
Optical galaxy counts vs. RM plots for the Perseus-Pisces supercluster chain

Two optical methods used: *Y. Xu, P. Kronberg, S. Habib & Q. Dufton ApJ 2006*

(a)

7°-smoothed galaxy column density vs RM

(used the 2MASS galaxy survey)



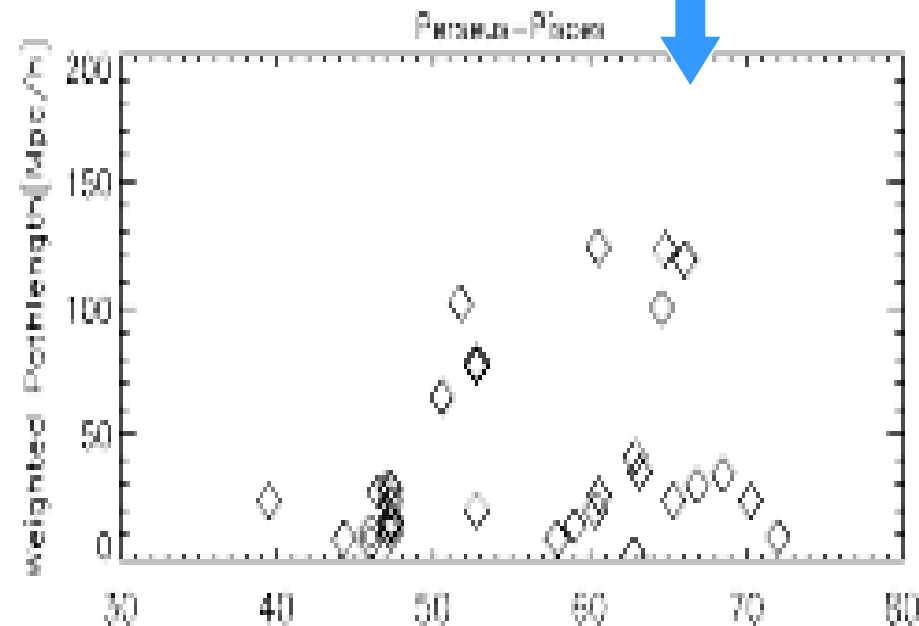
(b)

Weighted path length vs RM

(This used the CfA2 galaxy survey)

from 3-D Voronoi-tessilated IGM filament volumes
(\because 3-D spectroscopic z 's are measured).

also from 7°-smoothed data



Arecibo 305m Telescope, PR

An aerial photograph of the Arecibo 305m Telescope in Puerto Rico. The large, circular, segmented dish is the central feature, surrounded by dense green forest. A complex network of cables and a large spherical receiver are visible at the top of the dish. A tall, slender tower stands on the right side of the dish, with cables extending from it to the rim. The surrounding landscape is hilly and covered in lush vegetation.

*2 mm rms optics
illuminated area $\approx 200\text{m}$
uv overlap with DRAO $\approx 200\text{m}$*

Dominion Radio Astrophysical Observatory Penticton BC, Canada



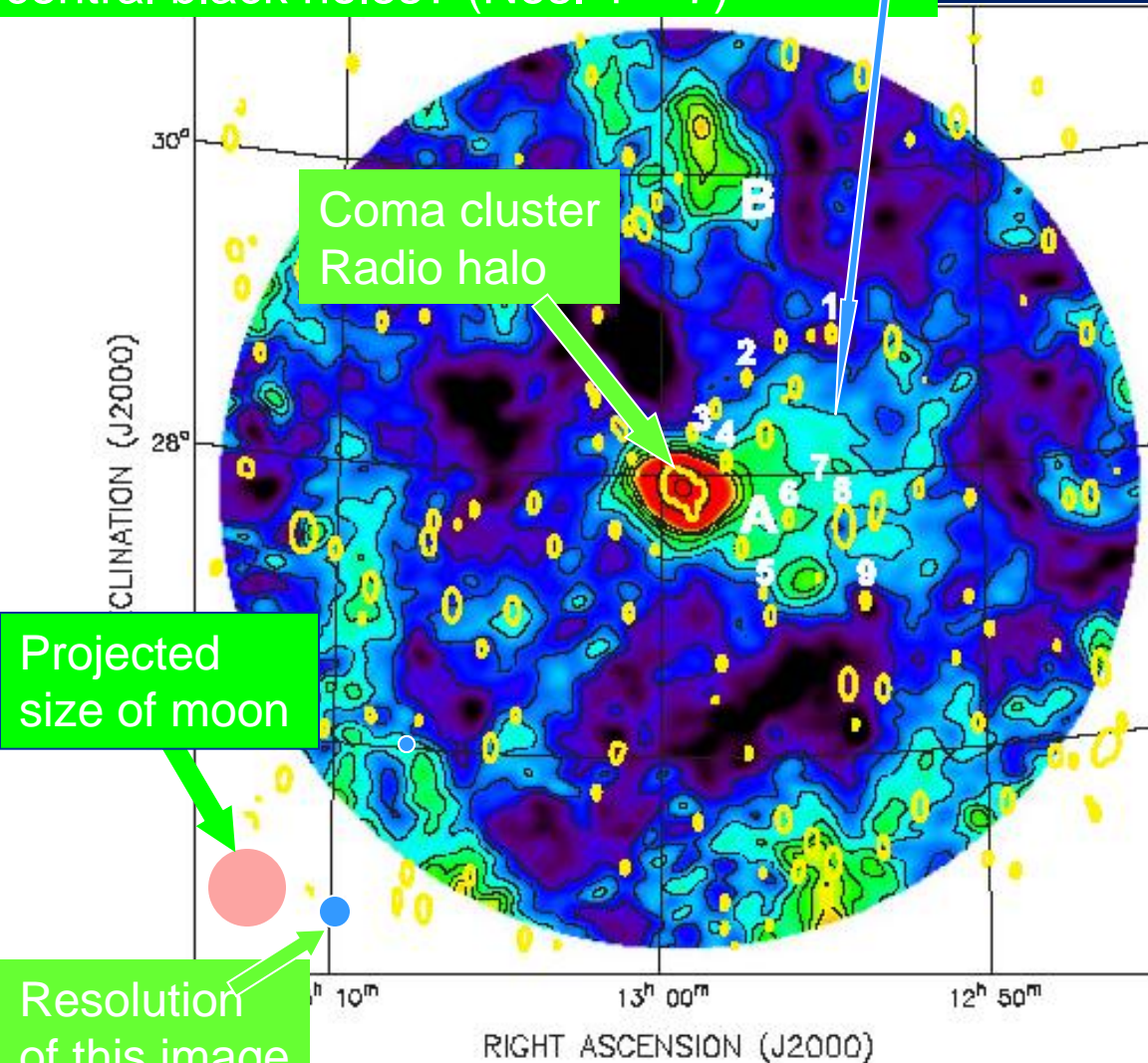
Max. separation = 617m \Rightarrow resolution equiv. to 1000m single dish. *Min. projected separation ≈ 18 m*

In 12 days, 1 full image within 9° circle at 408 MHz

COMBINED Arecibo-DRAO image, now smoothed to **10'** (Arecibo) resolution

P. Kronberg, R. Kothes, C. Salter, & P. Perillat ApJ 659, 267, 2007

Collective energization of several galactic
central black holes? (Nos. 1 – 7)



- Discrete sources removed,
- CMB + linear plane Milky Way foreground removed
- Strongest discrete sources re-overlaid (yellow ellipses)
- Black contours at 1.4, 1.9, 2.4, 2.9, 3.4, 3.9, 4.4, 10, 40K
- $\sigma \approx 250\text{mK}$ at 430 MHz

Region A (2 – 3 Mpc in extent)
requires a distributed “fresh”
energy source – plausibly
provided by the ~ 7 embedded,
radio galaxies.

$$Z_0 = \frac{3}{c} \beta$$

BH (magnetic + CR) energy output ($\gtrsim 10^{60}$ ergs) is “captured” within a few Mpc,

compare with

η (photons), $\approx 10\%$ of $M_{\text{BH}} c^2$ (not captured) appears comparable to η (CR + B),

2147+816 giant radio galaxy

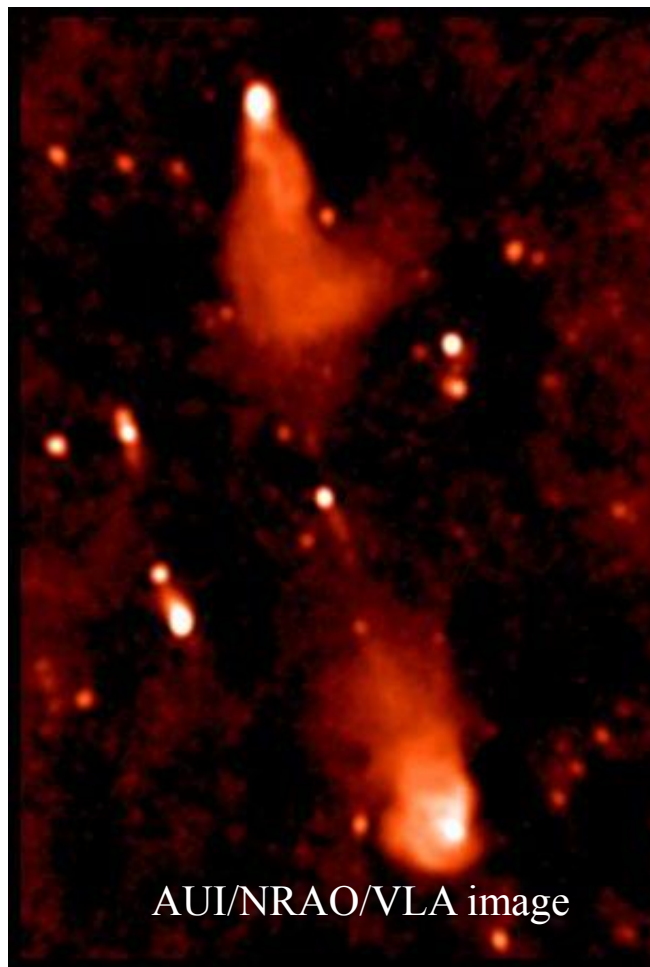
*Analysis of ≈ 70 GRG images
Kronberg, Dufon, Li, Colgate
ApJ 2001*

$z=0.146$

2.6 Mpc

*8 FR II-like GRG's, w. detailed,
multi- λ obs. & analysis
Kronberg, Colgate, Li, Dufton ApJL 2004*

- Willis & Strom, 1978,80
- Kronberg, Wielebinski & Graham. 1986,
- Mack *et al.* A&A 329, 431, 1998
- Schoenmakers *et al.* 1998,2000
- Subrahmanian *et al.* 1996
- Feretti *et al.* 1999
- Lara *et al.* 2000
- Palma *et al.* 2000



AUI/NRAO/VLA image

Magnetic fields in cosmic voids

1. Gamma ray cascades

Papers by: A. Noronov,

I. Vovk,

A.M. Taylor,

Elyiv

2009- 2012

2. Magnetoplasma diffusion from void galaxies, and from surrounding “filament” galaxies

A.M. Beck, H. Lesch et al. A&A 2013, in press



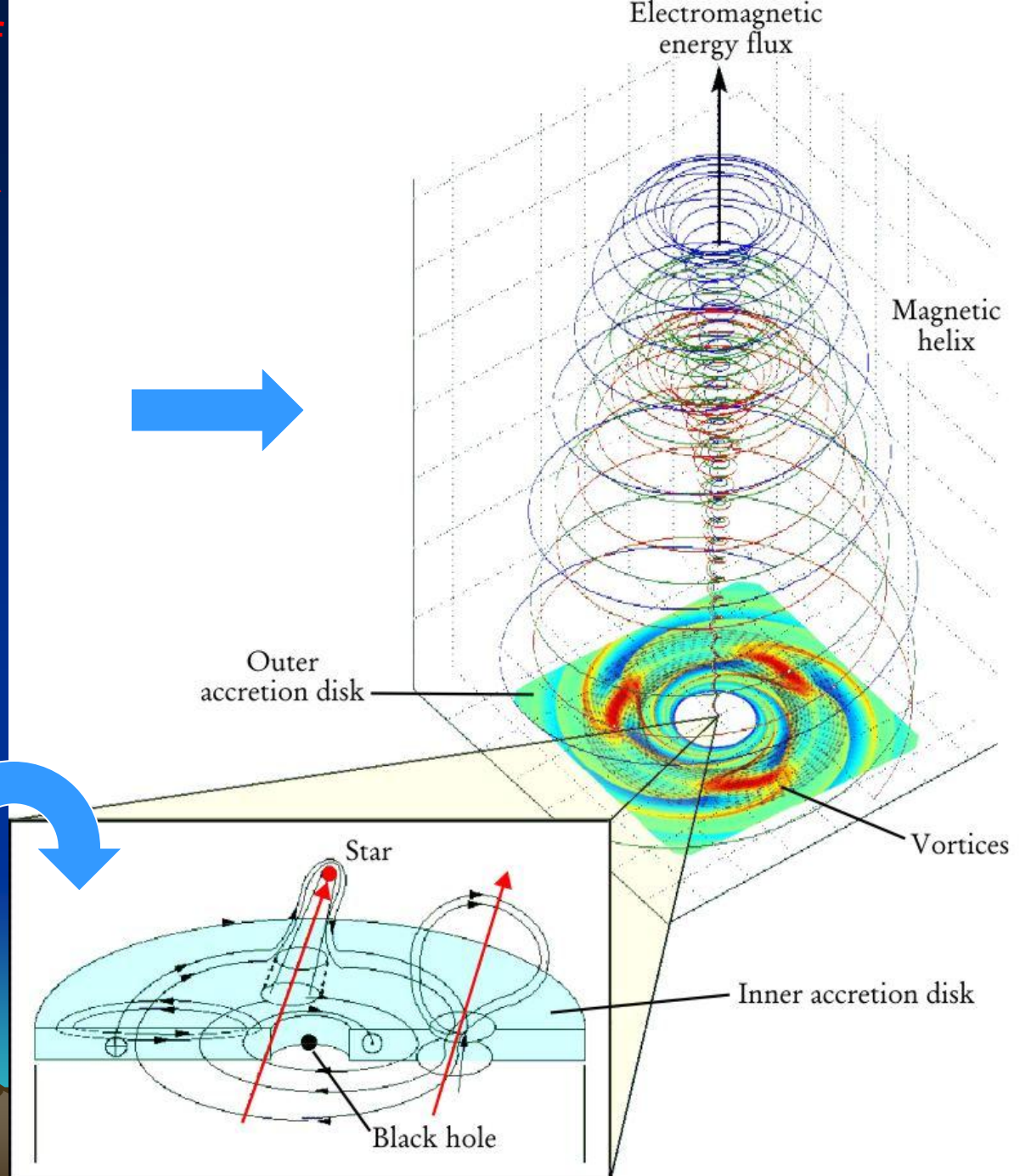
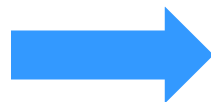
“Los Alamos” suite of models for BH infall energy release into a Poynting flux-dominated jet

S. Colgate, H. Li,
V. Pariev, 2001

Phys. of Plasmas
8, 2425

Li, Colgate,
Wendroff, Liska
2001 ApJ 551, 874

Accretion disk
dynamo
(S.A. Colgate)



Simulated magnetic tower jet/lobe in a cluster environment

M. Nakamura, I.A. Tregillis, H. Li, S. Li ApJ 686 843, 2008

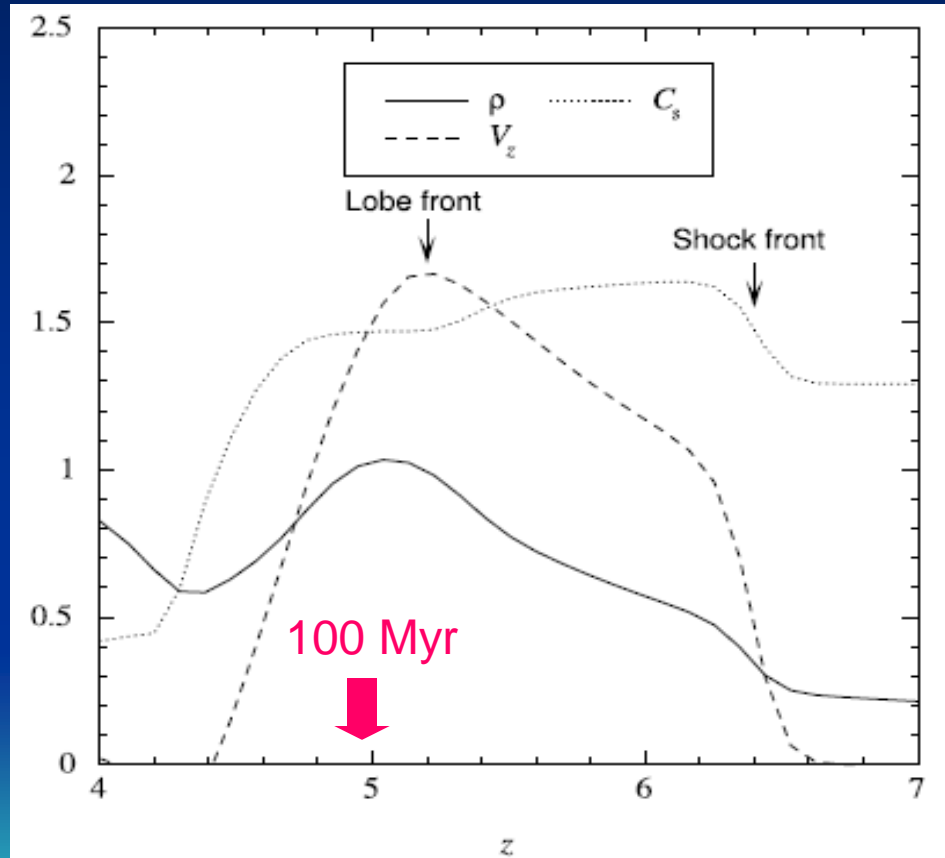
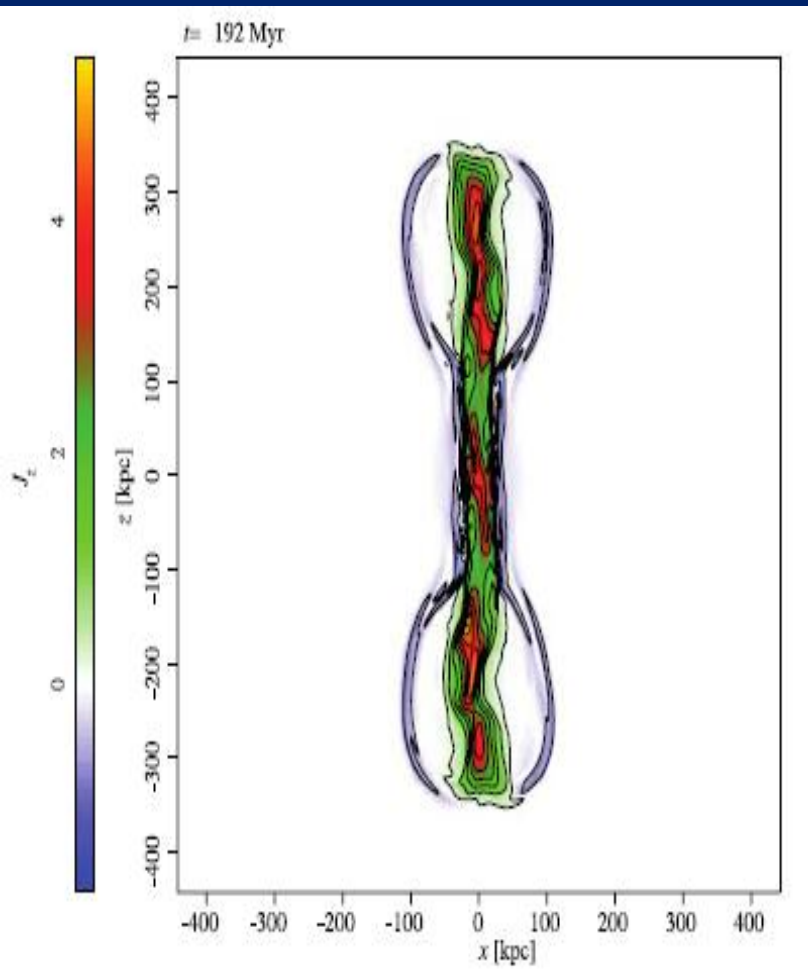
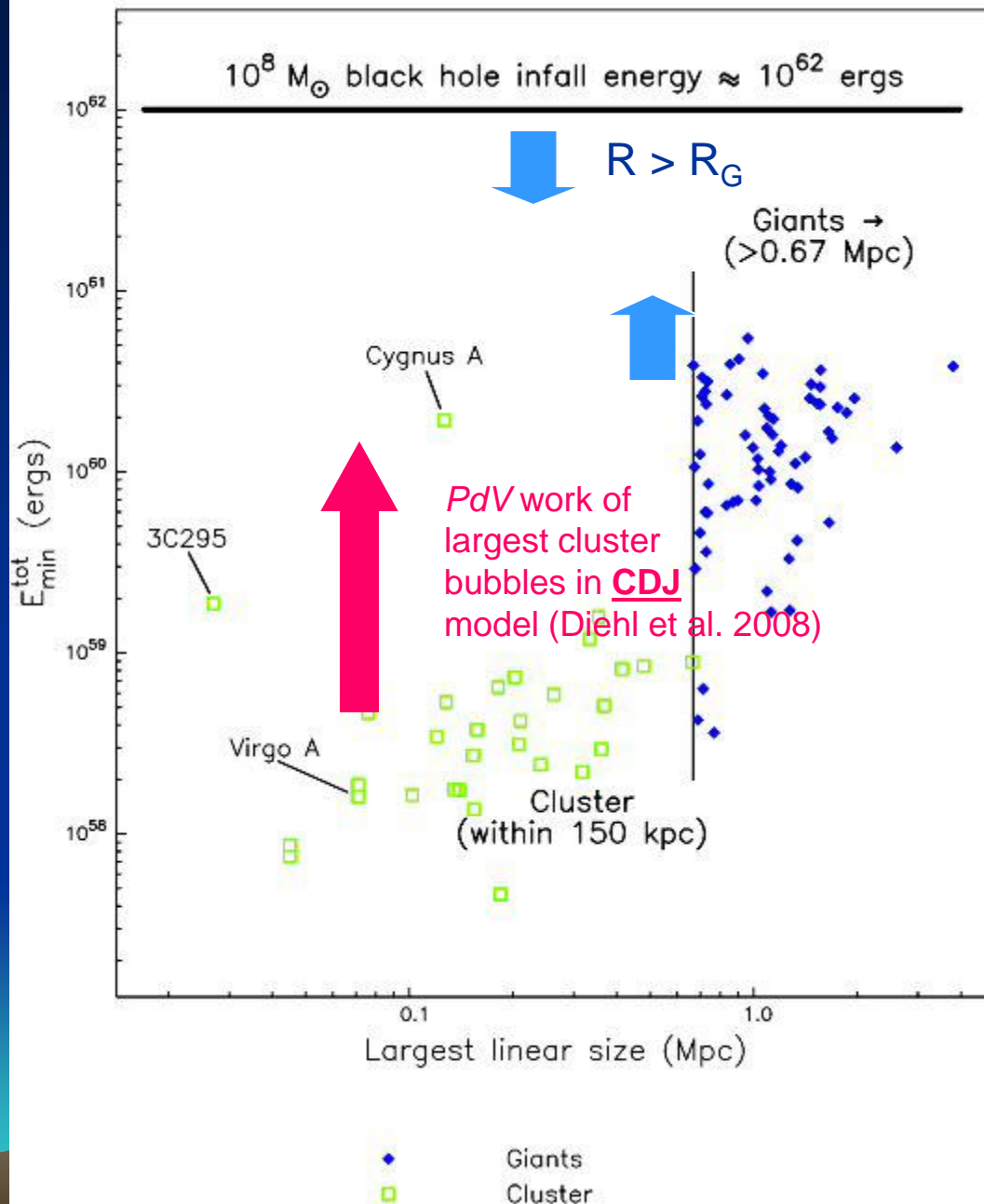


FIG. 2.— Axial profiles of physical quantities along the z -axis at $t = 3.0$ ($t = 72$ Myr): density ρ , sound speed C_s , and the axial velocity component V_z . The positions of the expanding shock and lobe fronts are shown.



$$=M_{\text{BH}}c^2$$

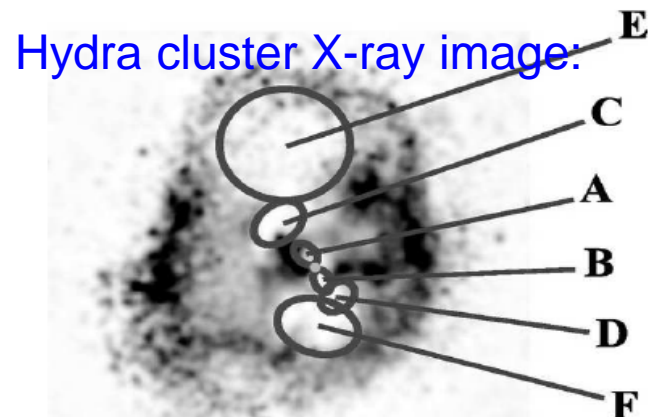


Mind the gap!!

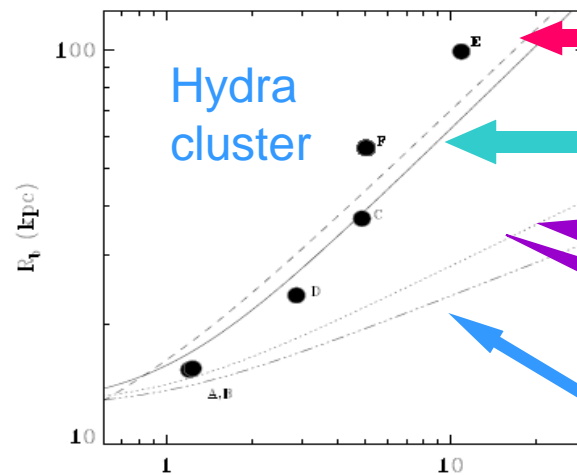
Accumulated energy
($B^2/8\pi + \epsilon_{\text{CR}}$) \times (volume)
from ``mature'' BH-powered
radio source lobes

GRG's
capture the highest fraction
of the magnetic energy
released to the IGM

*Kronberg, Dufton, Li, &
Colgate,
ApJ 560, 178, 2001*



Wise, M.W., McNamara, B.R., Nulsen, P.E.J., Houck, J.C., & David, L.P. *ApJ* 659, 1153, 2007



S.Diehl, H. Li, C.Fryer, D. Rafferty 2008 *ApJ*

CIH continuous injection hydrodynamic model - - -

CDJ current-dominated MHD jet model —

FML Bubbles contain frozen-in mag. loops

AD $\Gamma=5/3$, AD $\Gamma=4/3$
Adiabatically expanding hydrodynamic models

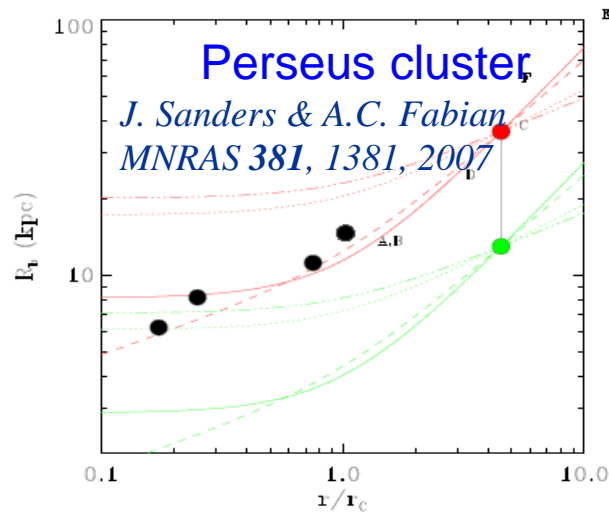


FIG. 7.— Bubble sizes for Perseus as a function of distance to the center. Lines as in Figure 6. The red data point shows the upper limit for the new bubble size estimate, the green data shows a lower limit. The correct answer will likely lie somewhere in between these two extremes.

limits to the true location of the bubbles. This will not only affect the radii themselves, but also the point at which other quantities are evaluated at, like density, temperature and pressure. In general the temperature rises outward in these systems, thus the temperature at the location of the bubble is likely to be systematically underestimated. The density and ambient pressure on the other hand will always be overestimated. This also means that any rise times derived from using the projected radius rather than the true distance to the center will result in estimates for the rise times that are systematically too low. We also note that the smaller the observed radius is, the higher the probability that it is due to an effect caused by projection.

But there are more subtle effects that projection has on our data. As we do not have an automated tool to detect bubbles, one has to rely on human experience in finding and identifying these systems. This task is much more difficult, if the cavities overlap with the bright cluster center or the bubble on the opposite side of the cluster. In fact, our sample does not contain *any* cavity system in which the bubble size exceeds the projected distance to the center, the slope of which is shown by the black solid line in Figure 8, even though this is statistically very improbable. This suggests that our sample is affected by what we will refer to as a “geometric” selection effect, introduced by our manual detection process.

Effects of Sig/Noise and projection effects;

Enßlin & Heinz
A&A 384, L27, 2002

Extragalactic jets as (V/U)HECR accelerators

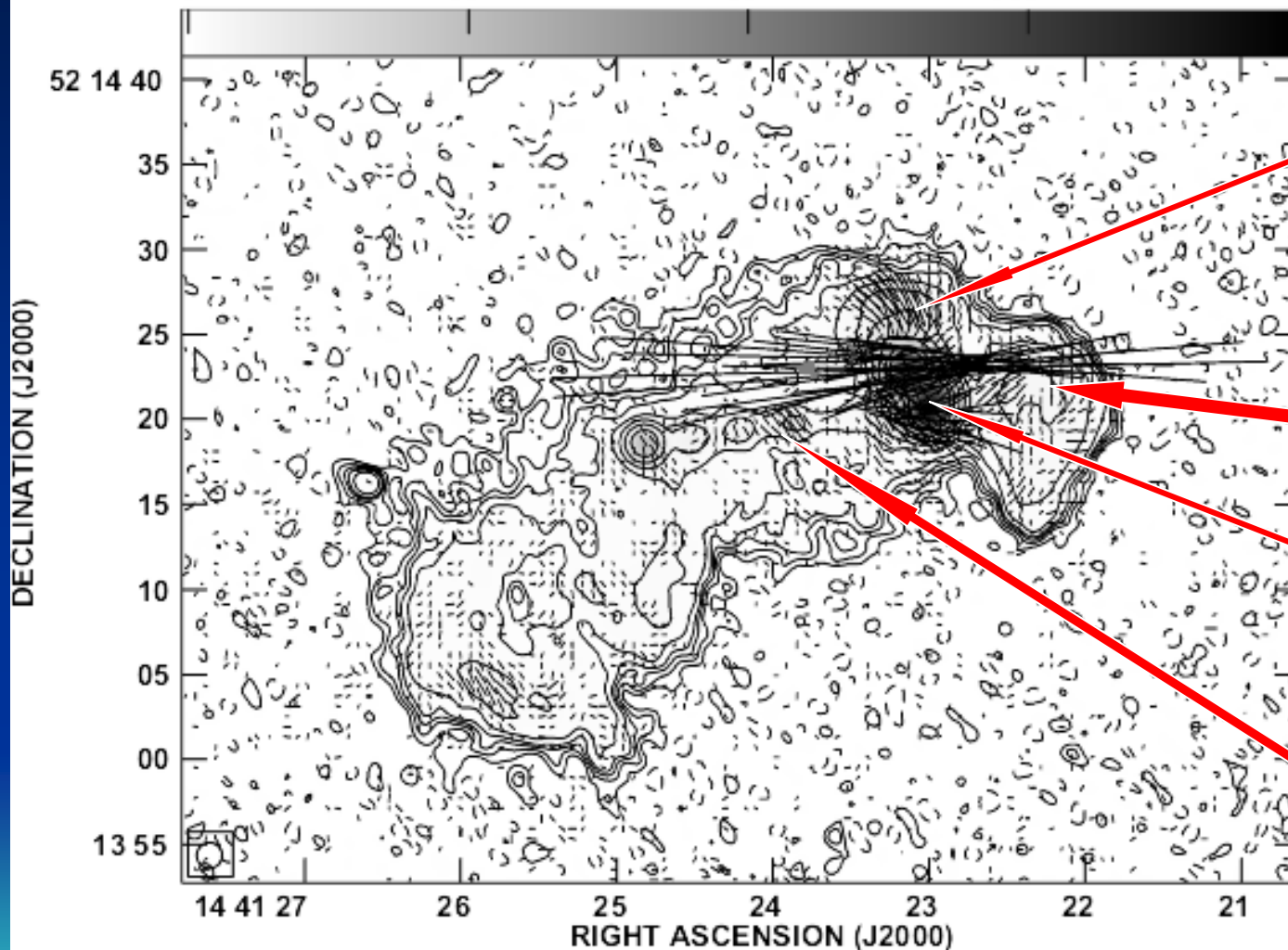


3C303 1.4GHz

PLot file version 5 created 02-MAY-2011 18:51:05

ALL: 3C303 IPOL 1406.750 MHZ 3C303L.ICL3.1

0 100 200 300



Grey scale flux range= -1.3 395.7 MilliJY/BEAM

Cont peak flux = 3.9566E-01 JY/BEAM

Levs = 5.000E-04 * (-1, 1, 2, 3, 4, 6, 12, 24, 48, 100, 200, 300)

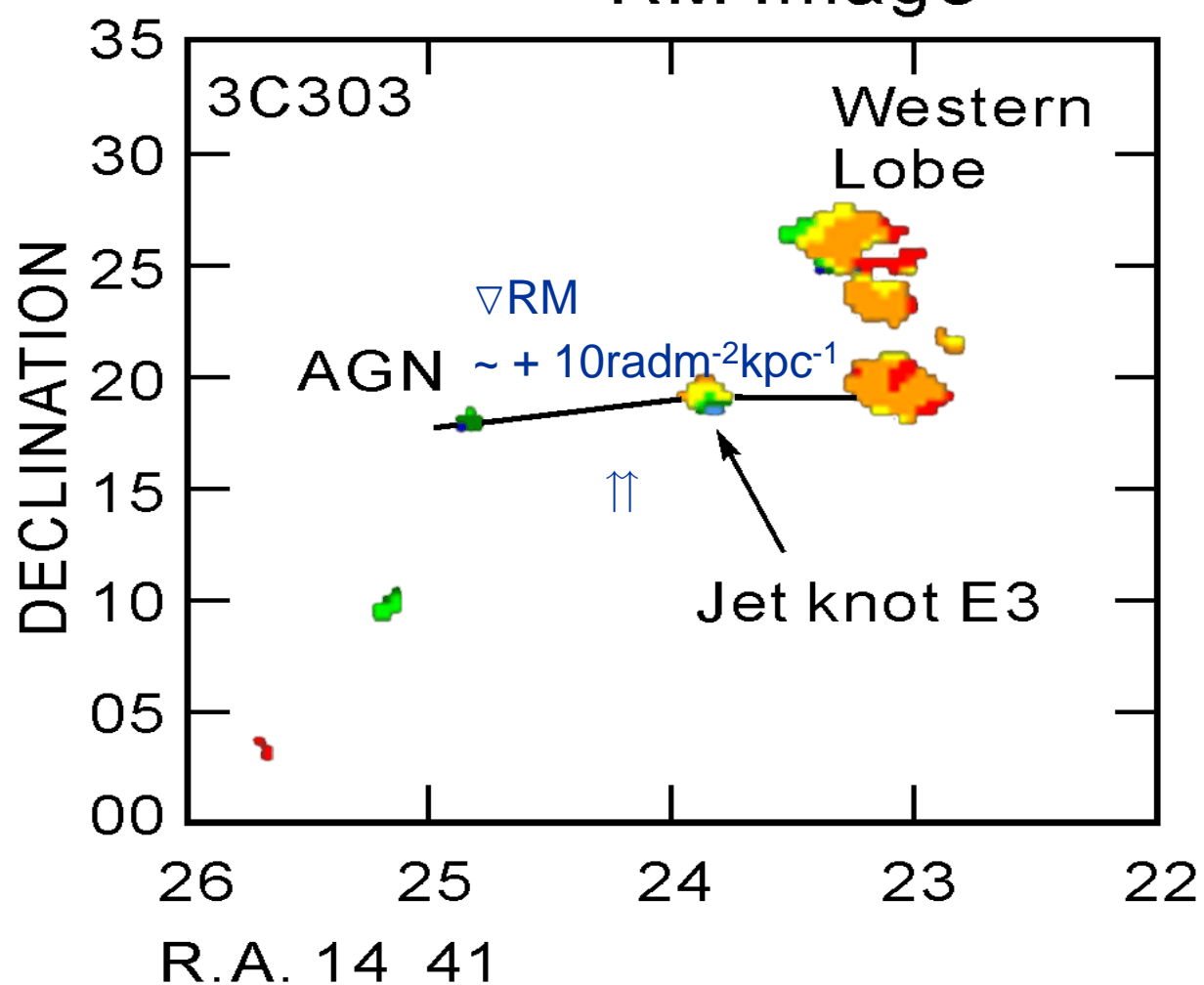
Pol line 1 arcsec = 2.5000E-03 JY/BEAM

3 spheroid "islands"
Each has high
B – ordering
& current signatures

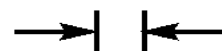
jet continues
undeflected
to here

jet disruption
point

Knot "E3" has a
measured ∇ RM
vector

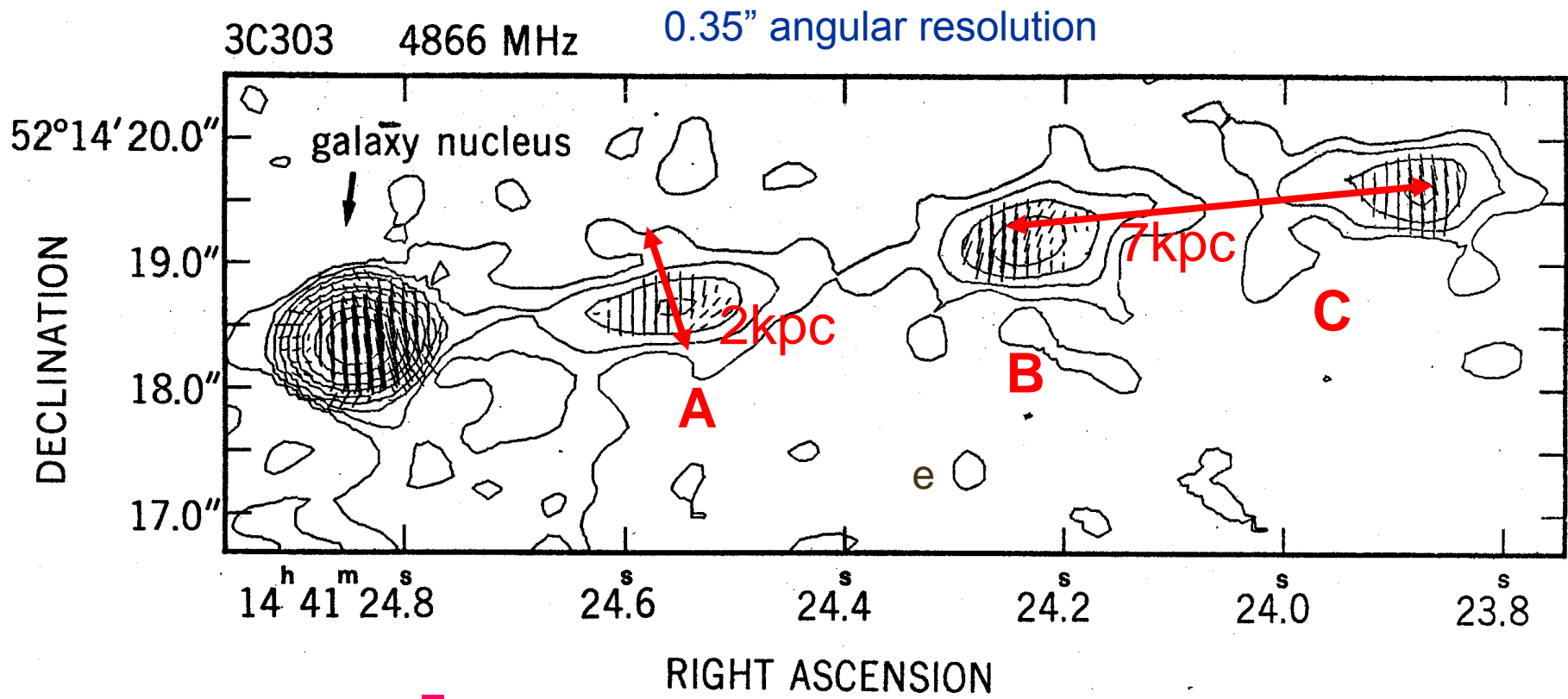


-20 -10 0 10 rad/m^2

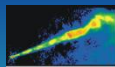


Foreground RM
Correction uncertainty

VLA image



Compare scales!



M87 jet on the physical scale of 3C303

M87 knot cocoons are ~ 12,000 times smaller than those in 3C303!
SMBH-powered jets are very scale-independent systems!

Analysis gives straightforward electrical circuit analogues for BH energy transfer into ``empty'' space

P.P. Kronberg, R.V.E. Lovelace, G. Lapenta & S.A. Colgate
ApJL 741, L15 2011

and

R.V.E. Lovelace, S. Dyda & P.P. Kronberg
Proc. Xth International Conf.on Gravitation, Astrophysics, and Cosmology:
Ed. Roland Triay 2012 *LA-UR 12-01129*

- $P \sim 10^{37}$ watts of directed e.m. power, and $I = 3.3 \times 10^{18}$ ampères of axial current
 sign of ∇RM gives I direction – in this case away from the BH
- Jet's electrical properties: (voltage, impedance, current)

$$I_0 = cr_2 B_{\phi(r_2)} = \frac{V_0}{Z_0} \approx 3 \times 10^{18} \text{ Amps (MKS)}$$

$$Z_0 = \frac{3}{c} \beta \text{ (cgs)} = 90 \beta \text{ Ohms (MKS)}$$

$$V_0 = \frac{r_0 B_0}{3^{1/4} \sqrt{R}} = 2.7 \times 10^{20} \text{ Volts (MKS)}$$

$$\frac{U}{c}$$

$\beta = \frac{U}{c} \lesssim 1$, and r_1, r_2 are the inner & outer transmission line radii (Lovelace & Ruchi, 1983)

Concluding Remarks

- We examine the implications of the excess of events seen towards the nearby radio galaxy Centaurus A, ASSUMING 1. ALL PROTONS, and 2. THAT ALL ORIGINATE AT Cen A
- OUR MODEL FRAMEWORK IS A “TIP OF THE ICEBERG” ANALYSIS, WHICH IS SET UP TO PRODUCE A VARIETY OF OTHER MODELS WITH ASSUMPTIONS OTHER THAN 1. AND 2. ABOVE
- OTHER, LARGE SCALE, ISOTROPIES ALSO APPEAR TO EXIST IN THE CURRENT AUGER DATA These point to the potential to finally address both the particles' origins, and properties of the nearby EGMF
- The angular distribution of events constrains the EGMF strength within several Mpc of the Milky Way, and implies that $\langle B_{IG} \rangle > 10$ nG.
- These results serve as pathfinders to future extensions of the above analyses:
e.g.
 - UHECR scattering from much more distant sources
 - Propagation time delays ($\sim 10^{4-5}$ yr to Cen A) for transient sources
 - The use of CR magnetic lensing signatures to attain tighter B_{IGM} constraints
 - Others

Extragalactic jet-lobe sources as electrical circuit analogues

Kronberg, Lovelace, Colgate *ApJL* 2011

Upcoming papers:

Lovelace & Kronberg *MNRAS submitted*

Lovelace & Richardson *in prep*



End

Philipp Kronberg

